

THE PENNSYLVANIA STATE UNIVERSITY  
SCHREYER HONORS COLLEGE

DEPARTMENT OF ENGINEERING SCIENCE AND MECHANICS

THE CHEMICAL EXFOLIATION OF HEXAGONAL BORON NITRIDE FOR  
RADIATION DETECTORS

MICHAEL KELLY  
SPRING 2013

A thesis  
submitted in partial fulfillment  
of the requirements  
for a baccalaureate degree  
in Engineering Science  
with honors in Engineering Science

Reviewed and approved\* by the following:

Joshua A. Robinson  
Assistant Professor of Materials Science and Engineering  
Thesis Supervisor

Barbara A. Shaw  
Professor of Engineering Science and Mechanics  
Honors Adviser

Judith A. Todd  
P.B. Breneman Department Head Chair  
Professor, Department of Engineering Science and Mechanics

\* Signatures are on file in the Schreyer Honors College and Engineering Science and  
Mechanics Office

## **Abstract**

This project entailed the synthesis and characterization of hexagonal boron nitride (h-BN) nanosheets via chemical exfoliation. The exfoliation procedure involved the bath sonication of h-BN powders in various solvents, followed by centrifugation. Nanofilms were prepared by means of spin coating and drop casting onto Si-based substrates. Using characterization techniques such as Atomic Force Microscopy (AFM), Scanning Electron Microscopy (SEM), and Dynamic Light Scattering (DLS), h-BN particle sizes were measured. This report effectively shows the promotion of h-BN agglomeration by ultrasonication and IPA.. Additionally, this report shows evidence that DMF is the best solvent for h-BN dispersion during chemical exfoliation.

Included in this report are the methods of exfoliation, characterization data from the fore mentioned techniques, and applications for radiation sensing.

# Table of Contents

<b>Abstract.....</b>	<b>i</b>
<b>List of Figures.....</b>	<b>iv</b>
<b>List of Tables.....</b>	<b>vi</b>
<b>Acknowledgements.....</b>	<b>vii</b>
<b>1 Introduction.....</b>	<b>1</b>
<b>2 Experimental Setup.....</b>	<b>3</b>
2.1 General Chemical Exfoliation Procedure.....	3
2.2 Substrate Surface Cleaning and Preparation.....	4
2.3 h-BN Thin Film Deposition.....	5
<b>3 Characterization Methods.....</b>	<b>7</b>
3.1 Optical Microscopy.....	7
3.2 Atomic Force Microscopy.....	8
3.3 Optical Profilometry.....	9
3.4 Dynamic Light Scattering.....	13
3.5 Concentration Evaluation with OHAUS Microbalance .....	16
3.6 Ultraviolet-visible Spectroscopy for Concentration Evaluation .....	19
3.7 X-ray Photoelectron Spectroscopy.....	21
<b>4 Results and Discussion.....</b>	<b>22</b>
4.1 Solvent Comparison.....	22
4.2 Sonication Impact on h-BN Particle Size.....	26
4.3 Sonication Time and Particle Agglomeration.....	30
4.4 h-BN Concentration vs. Particle Agglomeration .....	32

4.5 Solvent Impact on Particle Agglomeration .....	35
4.6 Centrifugation and h-BN Particle Size.....	37
4.7 Boron Nitride Starting Powder Evaluation .....	41
<b>5 Applications and Future Work.....</b>	<b>45</b>
5.1 Radiation Sensing.....	45
5.2 Acid Intercalant Exfoliation.....	47
<b>6 Conclusions.....</b>	<b>50</b>
<b>Bibliography.....</b>	<b>53</b>

## List of Figures

2.1: Ultrasonic Bath Schematic.....	3
2.2: M4L Plasma Etch.....	5
2.3: Vacuum Spin Coater.....	6
3.1: Deposition Comparison.....	7
3.2: h-BN on Si: Optical Profilometry.....	11
3.3: h-BN on SiO <sub>2</sub> : Optical Profilometry .....	11
3.4: Dynamic Light Scattering Precision.....	14
3.5: Dynamic Light Scattering Accuracy.....	15
3.6: SEM Comparison for DLS.....	15
3.7: Concentration Evaluation Charts.....	18
3.8: Superimposed Concentration Evaluation.....	19
4.1: h-BN Supernatants.....	23
4.2: Zoom of h-BN-IPA Suspension.....	24
4.3: Drop Casted Samples by Solvent.....	25
4.4: h-BN 26 1: SEM.....	27
4.5: h-BN 26 3: SEM .....	28
4.6: h-BN 26: DLS Charts.....	29
4.7: DLS Chart: 12 Hour Sonication.....	31
4.8: SEM: 12 Hour Sonication.....	32
4.9: h-BN 26 Test Tubes.....	33
4.10: h-BN 26 Controlled Concentration: DLS.....	34
4.11: h-BN in DMF and IPA: SEM.....	36

4.12: h-BN in IPA: DLS.....	37
4.13: h-BN 27 1&2: SEM.....	38
4.14: h-BN 27 3: SEM.....	39
4.15: h-BN 27 1&2: AFM .....	40
4.16: h-BN 27 1&2 Step Heights.....	40
4.17: h-BN 27 3 Step Height.....	41
4.18: Starting Powder Suspensions.....	42
4.19: Drop Casted Samples: Powder Comparison.....	44
5.1: Percent Change: XPS.....	46
5.2: Acid Intercalation Exfoliation: SEM.....	48
5.3: Acid Intercalation Exfoliation: AFM.....	49

## List of Tables

3.1: Recommended Probes.....	9
3.2: h-BN on Si: AFM.....	11
3.3: h-BN on SiO <sub>2</sub> : AFM.....	12
4.1: Concentration and Percent Yield by Solvent.....	23
4.2: Sonication and Centrifugation Info: h-BN 26.....	26
4.3: Concentration and Percent Yield by Sonication Time .....	33
4.4: Sonication and Centrifugation Info: h-BN 27.....	38
4.5: Concentration and Percent Yield by Starting Powder.....	43

## **Acknowledgements**

I would like to thank my research advisor, Dr. Joshua Robinson, for allowing me to work in his group for the past 2 years and providing support throughout this entire process. I would also like to thank some of the graduate students in my group, specifically Maxwell Wetherington and Ganesh Bhimanapati, for helping me with characterization assistance. Lastly, I would like to thank my honors advisor, Dr. Barbara Shaw, for supporting me with this project.



## Chapter 1

### Introduction

Recently, much attention has been focused on the extraction of single-layer graphene sheets due to the excellent electrical, thermal, chemical, and mechanical properties of this material [1]. As the isoelectric analogue to graphite, hexagonal boron nitride (h-BN) has likewise garnered significant interest as well. Unlike graphene though, h-BN has a wide band gap, making it an insulator as opposed to a semiconductor. As well as having a large band gap, h-BN also possesses excellent optoelectronic properties, high thermal conductivity, and good chemical inertness [1]. So far, previous investigations regarding h-BN have focused on the preparation of BN nanoparticles and nanofilms using predominantly physical/chemical vapor deposition, as well as solution-based and solid state methods. However, the chemical exfoliation of h-BN powders has been relatively unexplored to date. Wet oxidation methods, which are very common for graphene exfoliation, have been considered not as practical for h-BN due to its oxidation resistance [2]. Recently though, several exfoliation experiments have included the bath sonication of h-BN powders in multiple solvents. The question still remains though, as to what chemical method is most efficient in exfoliating h-BN powders with the highest concentration yield and most practical features.

Within the past few years, several experiments have been performed to exfoliate h-BN powders into few-layered and even monolayered nanosheets. Much of these experiments have included the mixing of h-BN starting powders with a strongly polar organic solvent, followed by a sonication/centrifugation procedure.

At this point, the main interest is to continue to find exfoliation methods that are effective in extracting single layer nanosheets. Moving forward, the critical goal revolves around finding the most effective method for synthesizing high quality, controllable suspensions of h-BN.

## Chapter 2

### Experimental Setup

#### 2.1 General Chemical Exfoliation Procedure

To begin the chemical exfoliation procedure, h-BN starting powders were measured out to various desired masses and dispersed into 45 ml of solvent. For these experiments, several solvents were used, notably Isopropyl Alcohol (IPA), Dimethylformamide (DMF), and Deionized water (DI Water). To aid in the dispersion process and to begin the exfoliation, the suspensions were placed into an ultrasonic bath. During this process, piezoelectric transducers, located at the bottom of the bath, produced ultrasonic waves that passed throughout the water. In doing so, the h-BN suspensions were disrupted via mechanical agitation, thus beginning the chemical exfoliation. The diagram below provides a visual description of the sonication bath setup and the components involved.

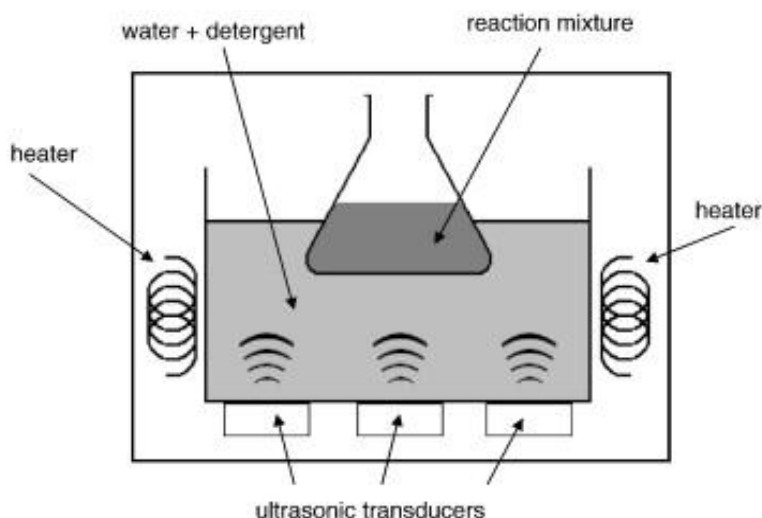


**Figure 2.1:** Diagram of ultrasonic bath used for chemical exfoliation with labeled components [3].

Sonication times for these experiments varied significantly, and will be further discussed in later sections. Following the sonication process, the h-BN suspensions were then centrifuged at various angular speeds and times. After completion of centrifugation, and depending on the nature of the exfoliation process, the resultant h-BN supernatants were sometimes filtered using filter papers with pore sizes ranging from 5-10  $\mu\text{m}$ . The insertion of the filtering process was decided based on the desired final boron nitride particle size. At this point, the exfoliation procedure was complete, and the ensuing suspensions were ready to be deposited for characterization.

## **2.2 Substrate Surface Cleaning and Preparation**

Once the exfoliation procedure was complete, the deposition process could begin. This began with preparing the substrates via surface cleaning techniques. First, to begin the cleaning, the substrates were submerged in acetone in an ultrasonic bath for at least thirty seconds. They were then immediately transferred into a petri dish filled with IPA to remove the acetone. Finally, they were transferred once more into DI Water, and then dried with a nitrogen gun. Once this initial cleaning process was complete, the substrates were then plasma etched with oxygen gas. The purpose of the plasma etch was to continue the surface cleaning and to also increase the hydrophilic nature of the substrate [4]. Figure 2.2 below shows the plasma etcher used for substrate cleaning in this project. Once the plasma etching was complete, the substrates could be used for deposition.



**Figure 2.2:** Image of M4L Plasma Etcher used for substrate cleaning during sample preparation [4].

## 2.3 h-BN Thin Film Deposition

Several methods were used for depositing thin films. Generally, these methods were chosen based upon the concentration of the suspension and the desired array of h-BN particles for characterization. For this project, drop casting, spin coating, and dip coating methods were all used. However, the first 2 methods were the primary means of deposition, and so these will be the ones shown in this report. For drop casting, the h-BN suspensions were dropped, using transfer pipettes, onto silicon (Si), silicon dioxide ( $\text{SiO}_2$ ), or sapphire ( $\text{Al}_2\text{O}_3$ ). Depending upon the solvent and the time restraint, the evaporation process for the drop casting was at times assisted through the use of a hotplate. Again, temperatures varied by solvent. For DI water samples, the drop casting

was performed at temperatures up to 65 ° C, while the temperature was restricted to 35 ° C for DMF and IPA samples.

One of the issues regarding drop casting is the concentrated agglomeration of particles following evaporation. Spin coating, on the other hand, eliminates some of these issues by depositing films with more isolated particles. The issue with spin coating though lies in the fact that the h-BN suspension needs to be relatively high in order to get decent surface coverage. Therefore, when creating a thin film, this method was reserved for suspensions with concentrations of at least .40 mg/ml. Figure 2.3 provides a visual of the spin coating instrument that was used throughout this project for h-BN thin film deposition.



**Figure 2.3:** Vacuum spin coater used for sample deposition. Operates at rotational speeds from 500 rpm to 8,000 rpm.

## Chapter 3

### Characterization Methods

#### 3.1 Optical Microscopy

As previously mentioned, the difference between drop casting and spin coating deposition methods is generally in the particle array on the sample surface. Before doing any other surface characterization, Optical Microscopy was used to determine the surface coverage of the h-BN particles. The figure below displays a side-by-side comparison of the same suspension deposited 2 different ways. The sample on the left in Figure 3.1 was drop casted onto  $\text{SiO}_2$  at room temperature, while the sample to the right was deposited via spin coating at 2,000 rpm. As seen, the drop casting deposition technique provides much greater surface coverage compared to the spin coating. However, the h-BN particles become much more agglomerated in doing so.

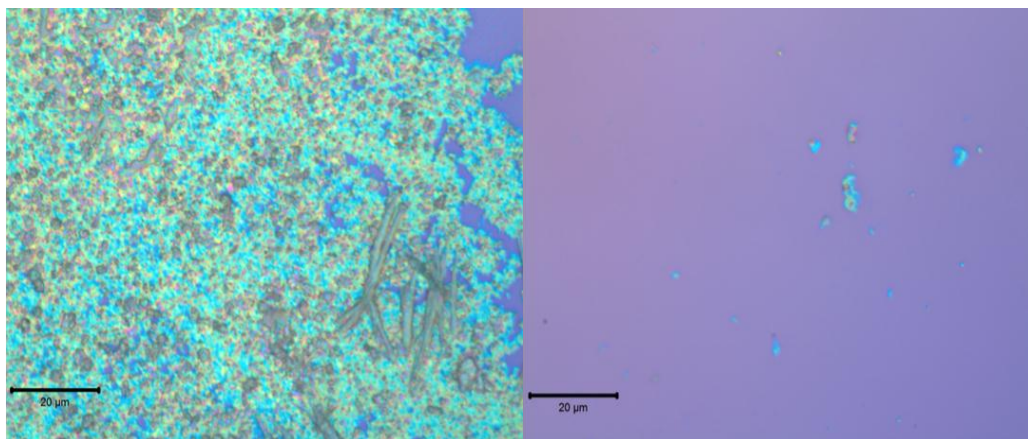


**Figure 3.1:** Suspension of h-BN in DMF deposited onto  $\text{SiO}_2$  via drop casting at room temperature (left) and spin coating at 2,000 rpm (right).

### 3.2 Atomic Force Microscopy

After film deposition, atomic force microscopy (AFM) was used for particle size characterization. In using this technique, the objective was to determine both lateral sizes and thicknesses of h-BN particles as they related to the specific exfoliation procedure. The capability to provide 3-dimensional topographic information of the h-BN films made this technique applicable for obtaining the desired surface profiling. Although high lateral resolutions on the range of 5-15 nanometers can be achieved using this instrument, there are also limitations involved that make this technique less inviting [5]. Specifically, the main problem associated with obtaining size distribution data from AFM is the small scan area. The particular instrument used for this project has a maximum X-Y scanning area of  $90\text{ }\mu\text{m}^2$  [5]. Therefore, for samples on the order of  $3\text{-}4\text{ cm}^2$ , this technique was not very effective in determining size distribution information for entire h-BN samples. Also, the software associated with this instrument does not have a distribution analysis feature, thus making it difficult to determine the allocation of h-BN particles without individually measuring isolated constituents. Therefore, this technique was primarily reserved for obtaining film thicknesses due to the fact that the other characterization techniques used did not have the capability to do so at high accuracy.

One other area of interest that this project attempted to explore was the relationship between h-BN particle sizes and certain mechanical properties, such as modulus, adhesion, and elasticity. With peak force quantitative nanomechanical (QNM) property mapping, this particular AFM instrument has the ability to provide characterization of nanoscale materials with an exceptionally wide range for modulus (approximately 1 MPa to 50 GPa) [6]. The principle of operation for this imaging mode is



based on a probe calibration technique that focuses on 3 material specific parameters. These parameters are deflection sensitivity, tip radius, and spring constant [6]. To begin this calibration procedure, the AFM probe scans across the h-BN sample at a significant peak force set point. The purpose is to achieve a sufficient deformation of at least 2 nanometers in order to gain measurements of the tip radius [6]. Because a certain level of deformation is required, the stiffness of the probe is of great significance. For this project, the probe stiffness was ultimately what caused this calibration procedure to be impractical. Bulk boron nitride, in the hexagonal structure, has a modulus in the range of 30-40 GPa. As shown in Table 3.1, this modulus requires the DNISP-HS probe in order to achieve necessary deformation. This particular probe has a diamond tip and costs over \$3,000. Therefore, the exceptional hardness of boron nitride makes this calibration procedure impractical, and thus the mechanical properties of h-BN were not studied in this project.

Sample Modulus (E)	Probe	Nominal Spring Constant (k)
1 MPa < E < 20 MPa	ScanAsyst-Air	0.5 N/m
5 MPa < E < 500 MPa	Tap150A, P/N MPP-12120-10	5 N/m
200 MPa < E < 2000 MPa	Tap300A (RTESPA), P/N MPP-11120-10	40 N/m
1 GPa < E < 20 GPa	Tap525A, P/N MPP-13120-10	200 N/m
10 GPa < E < 100 GPa	DNISP-HS	350 N/m

**Table 3.1:** Recommended probes for associated sample modulus and spring constant [6].

### 3.3 Optical Profilometry

In an attempt to overcome the limitations in the scan size of AFM, another surface profiling technique was explored to study the particle sizes of h-BN. This technique, optical profilometry, is a fast, non-contact surface imaging approach in which incident

light is split into 2 beams [7]. One beam shines upon the sample surface, while the other is sent to a reference mirror. The reflections of these beams are then combined and sent to a detector [7]. If interference occurs from differences in the 2 paths, information about the surface can be obtained. The main advantage of this approach is that large areas can be scanned at exceptional speeds. Although the micrometer lateral resolution is much less than that of AFM, this technique is valued more for its ability to attain fast data of millimeter-sized scan areas. The problem with this approach is that the index of refraction of the sample material differs from that of the substrate. With transparent materials, like boron nitride, this becomes an issue, as the substrate contributes to the reflected beam of light that the detector receives. To understand the effects of substrate interference, optical profilometry and AFM data was compared for h-BN films on silicon, silicon dioxide, and sapphire. A scribe mark was used to ensure that the same sample location was measured by both characterization techniques. Figure 3.3 (below) illustrates the optical profilometry scan area and corresponding height profile for h-BN on Si. The 3 measured lines show particle sizes on the order of approximately 2 nm. This same sample was then scanned using AFM. Table 3.1 shows the corresponding size data for 2 different scan areas of  $100\text{ }\mu\text{m}^2$ . As seen, the true mean particle heights range from 24-29 nm.

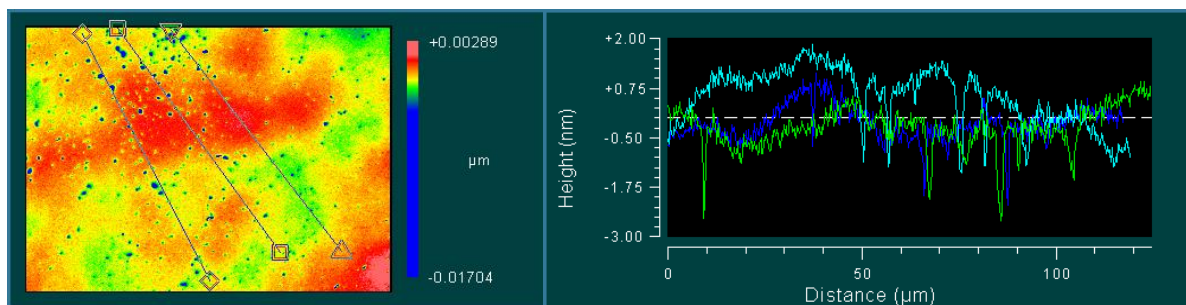


**Figure 3.2:** Height profile for h-BN on Si from optical profilometry. The values are underestimated in comparison to the true heights.

Site 1			Site 2		
201 Particles Averaged			273 Particles Averaged		
Site 1:	Parameter	Mean	Minimum	Maximum	Sigma
	Height	29.323 (nm)	3.604 (nm)	90.340 (nm)	13.450 (nm)
	Diameter	220.743 (nm)	110.193 (nm)	1206.704 (nm)	144.123 (nm)
Site 2:	Parameter	Mean	Minimum	Maximum	Sigma
	Height	24.247 (nm)	1.811 (nm)	70.839 (nm)	13.801 (nm)
	Diameter	199.162 (nm)	110.193 (nm)	906.001 (nm)	113.863 (nm)

**Table 3.2:** AFM data for h-BN on Si, evaluated at 2 sites. At each site, over 200 particles were measured for comparison to the corresponding optical profilometry data.

It is clear that the silicon substrate interfered with the reflected beam and caused an underestimation in the size of the h-BN particles. The same procedure was done for h-BN on silicon dioxide and sapphire.

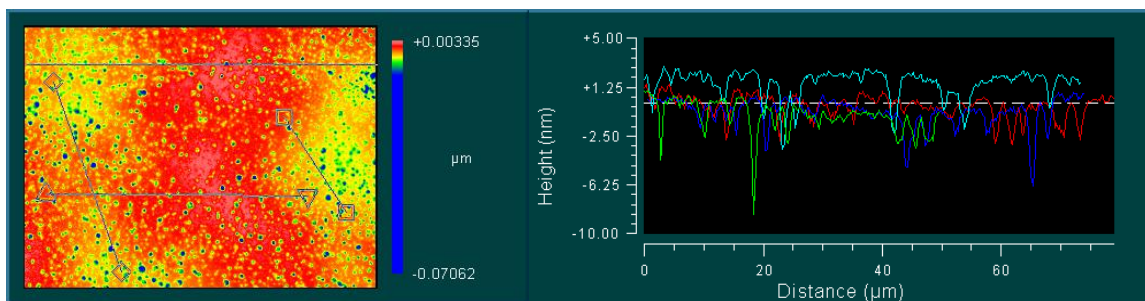


**Figure 3.3:** Height profile for h-BN on SiO<sub>2</sub> from optical profilometry. The values are underestimated in comparison to the true heights.

**Site 1:  
319 Particles Averaged**

Parameter	Mean	Minimum	Maximum	Sigma
Height	19.411 (nm)	4.775 (nm)	86.267 (nm)	11.674 (nm)
Diameter	176.263 (nm)	110.193 (nm)	1068.364 (nm)	89.711 (nm)

**Table 3.3:** AFM data for h-BN on SiO<sub>2</sub>. 319 particles were measured and averaged for comparison to the corresponding optical profilometry data.

Again, the data shows that the substrate interference has an effect on the measurement of particle heights. This time, the optical profiler measured the particles to be on the order of approximately 2-8 nm, as shown in Figure 3.3. AFM, on the other hand, averaged over 300 h-BN particles and obtained an average height of 19 nm (Table 3.3).

This same procedure was then performed for h-BN particles on sapphire substrates. This time, the size measurements between the 2 techniques were within 5% of each other, showing that the optical profiler is accurate when measuring h-BN particles on sapphire.

The results from this study can be attributed to the differences in the indices of refraction for h-BN and the respective substrates. Bulk h-BN has a measured refractive index of 1.8. Of the three substrates, sapphire (1.77) is the closest match to h-BN, which explains why there was no substrate interference in the optical profilometry data for h-BN on sapphire.

Even though this study has effectively proven that optical profilometry can be an accurate characterization method for acquiring particle sizing data for h-BN on sapphire substrates, there are several issues regarding this technique that make it difficult to trust. The main problem is the fact that agglomerated particles cannot be distinguished from

individual isolated particles. Due to the lower lateral resolution of this technique, there is no way to visually interpret the data in an accurate fashion. Therefore, although this method has the capability of obtaining fast data over large areas, it is too difficult to accurately analyze the data in a way that would make this technique practical for this project.

### 3.4 Dynamic Light Scattering

Thus far, all characterization has been performed on deposited thin films. Dynamic light scattering (DLS) is a characterization technique that measures nanoparticle sizes in suspension. The particular instrument used for this project, Malvern Nanosizer, is capable of measuring particles from .3 nm to 10  $\mu\text{m}$  [8]. The operating principal behind this technique is the Stokes-Einstein relationship, which relates the Brownian motion of particles to the intensity of scattered light [8]. During testing, laser light is shined through a suspension of h-BN particles in a given solvent. The Brownian motion of particles ultimately causes scattering of the laser light. The associated scattering intensities are then analyzed and the particle sizes are obtained via the Stokes-Einstein equation (below) [8].

$$D = \frac{k_B T}{6\pi \eta r}$$

In this equation,  $k_B$  is Boltzmann's constant,  $T$  is the temperature,  $\eta$  is the viscosity of the suspension, and  $r$  is the radius of the particle. Because this method ultimately measures a radius, it assumes that the particles are spherical ( $x=y=z$ ). For the boron nitride particles in this report, this is not necessarily the case, which presents a

caveat. For this reason, a comparative study was done between DLS and scanning electron microscopy (SEM) to determine the accuracy of this technique. Before doing so though, this technique was tested for its repeatability. To do this, the same h-BN suspension was tested 3 consecutive times, and the resulting data was compared.

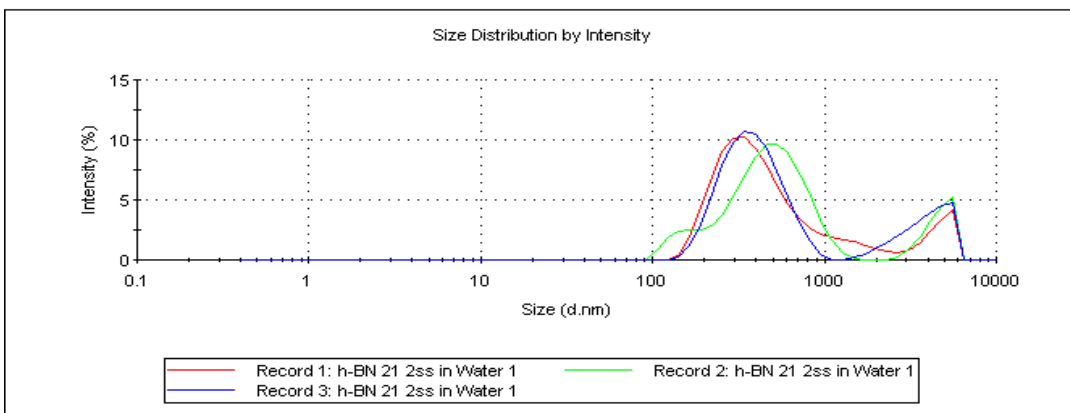


**Figure 3.4:** Size distribution chart from dynamic light scattering. This is based off of particle intensity percent of h-BN in DI water. 3 colors represent consecutive runs of the same suspension.

Figure 3.4 represents the high degree of repeatability for DLS measurements. The stability of this data concludes that this method can be trusted for its consistency.

Next, the caveat regarding the spherical nature of the particle needed to be addressed. To do so, DLS size distribution data was compared to measured particles in SEM. Figure 3.5 displays the size distribution of h-BN particles in water via intensity percent, as determined by dynamic light scattering. The results for the peak show a mean diameter of 475.5 nm. When compared to the visible h-BN particles shown in the SEM image in Figure 3.6, this seems to be an accurate measure. A majority of the h-BN particles appear to be on the order of approximately 500 nm laterally.

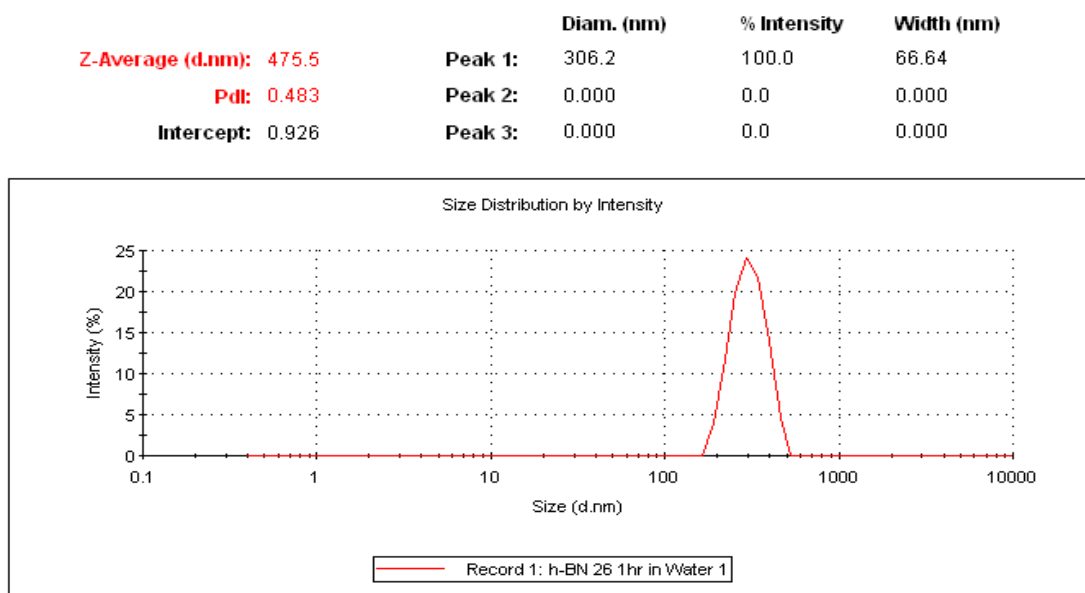


**Figure 3.5:** DLS size distribution intensity relationship of an h-BN suspension in water.

Measurements were repeated 3 times, as represented by the different colors.

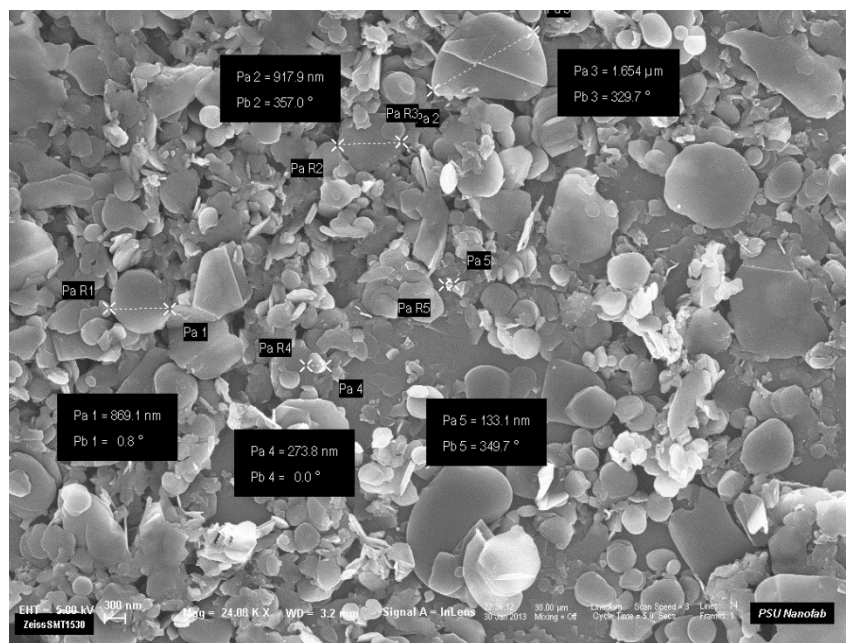


**Figure 3.6:** SEM image of same h-BN suspension from Figure 3.5, above. h-BN was drop casted onto silicon and sputtered with iridium before scanned.

From this comparison, it is concluded that DLS can be used as an effective means of characterization for particle size testing.

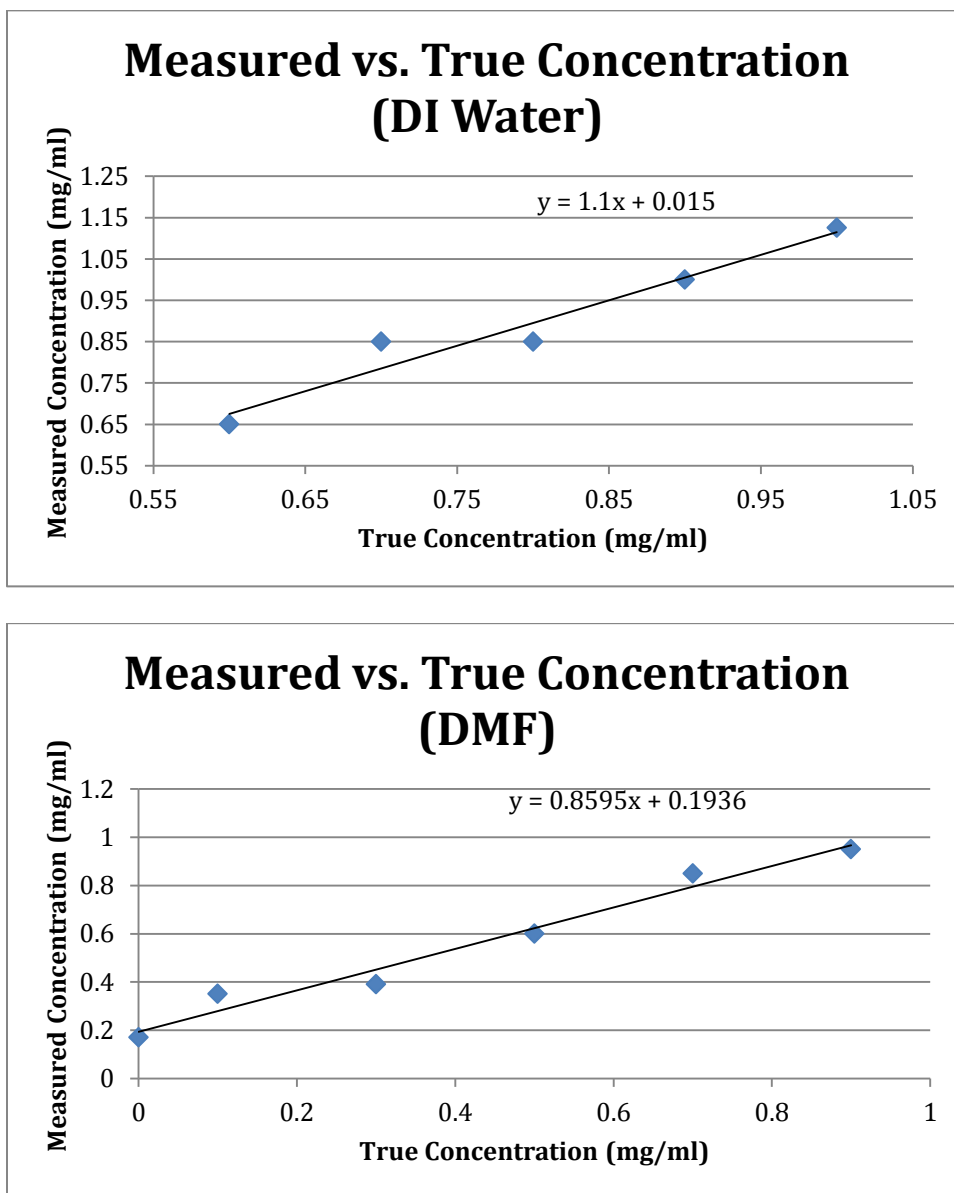
### 3.5 Concentration Evaluation with OHAUS Microbalance

One of the experiments performed in this project examined the effect of h-BN suspension concentration on particle agglomeration. Because of this study, it was necessary to be able to accurately measure the concentration of suspensions. Although the concentrations of the suspensions were initially known before exfoliation, they became unknown after the centrifugation step. When the suspensions were decanted to remove the precipitate, the amount of boron nitride in the resultant supernatant was unknown. Therefore, a method for determining the final h-BN concentration after exfoliation was essential to this project.

The method that was predominantly used throughout this project involved measuring out the boron nitride mass contained within a small volume of suspension. Specifically, 2 ml of h-BN solution was transferred into a small aluminum cup and placed on a hot plate at 100 °C. The mass of the cup was measured initially and then measured once more after complete evaporation of the solvent. The difference in mass was taken as the amount of boron nitride present in 2 ml of solution, thus allowing for the calculation of concentration. This method was performed first with concentrations of known value. However, in doing so, it was evident that this method generally overestimated the concentration by a small, yet noticeable degree. Because of this, a calibration procedure was set forth to determine a consistent factor of error that was inherent in performing this method. This procedure consisted of measuring 5 known h-BN concentrations using the same evaporation technique. This procedure was done separately for each of the 3 solvents. For DI Water, the 5 concentrations used were .6, .7, .8, .9, and 1.0 mg/ml. For DMF and IPA, the 5 concentrations used were .1, .3, .5, .7, and .9 mg/ml. In addition, a



control was measured, which consisted of just solvent without any boron nitride. The concentrations of these suspensions were calculated using the procedure that was previously described. Then, the calculated concentrations were plotted vs. the true concentrations. A first order linear fit was mapped to each of the plots.



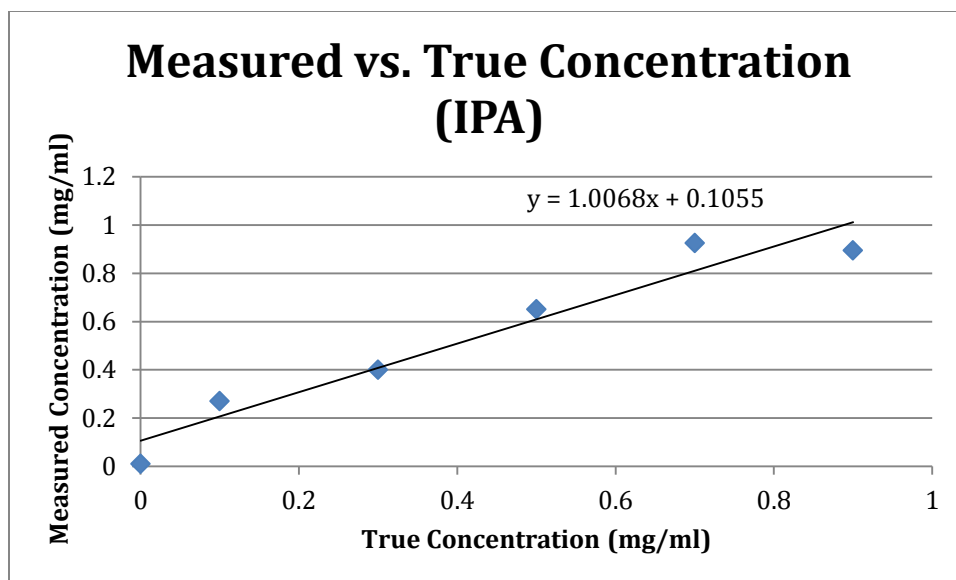


**Figure 3.7:** Plots of measured vs. true concentration for DI Water (top), DMF (middle), and IPA (bottom). These plots were used to measure concentrations of suspensions via extrapolation.

Figure 3.7, above, displays the first order, linear relationships between the measured concentrations and the true concentrations for each of the 3 solvents. These plots were used to extrapolate data in order to convert measured concentrations into true concentrations. Figure 3.8, below, shows the relationships of the 3 solvents superimposed on a single plot. Interesting to note here is that for all 3 of the solvents, this method returned a concentration value other than zero for the measurement of the pure solvents. This confirms the fact that when evaporating the liquid, whether it is pure solvent or an h-BN suspension, there is some residue left in the aluminum cup. Though the plot of the DI water nearly returns to zero, there is still a residual effect that needs to be accounted for, which is exactly what this evaluation method does.

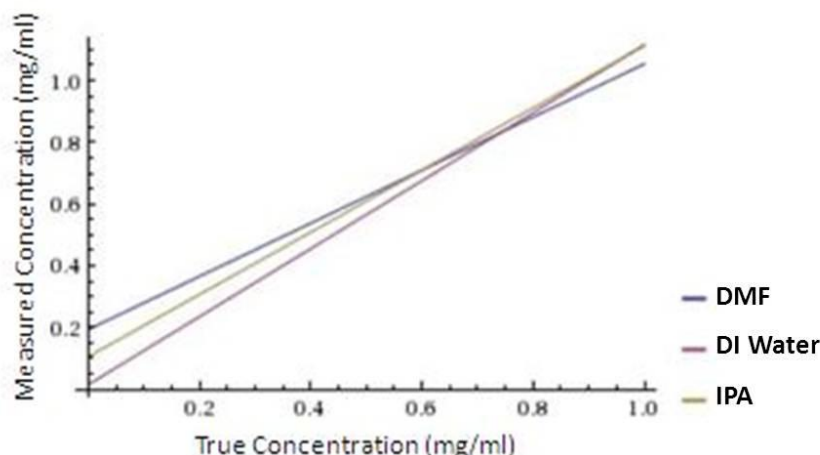


**Figure 3.8:** Superimposed plot of the measured concentration vs. true concentration relationships for each of the 3 solvents (DMF, DI water, IPA).

Thus, these plots were ultimately used to adjust for the overestimation error that is inherent when measuring concentrations using the microbalance. During the measurement process, the masses for the aluminum cups, both before and after evaporation, were measured 5 times and averaged to reduce error.

Once these relationships were determined, this method became very simple and fast, making it a desirable approach for concentration measurement.

### 3.6 Ultraviolet-visible Spectroscopy for Concentration Evaluation

Another method for determining the concentration of h-BN suspensions uses Ultraviolet-visible spectroscopy, or UV-Vis. This characterization method operates on the relationship between incident and transmitted light when passed through a solution. Specifically, this technique applies Beer's Law, shown below, to ultimately calculate the concentration of a solution [9].

$$\log(I_o/I) = \epsilon Lc$$

where  $I_0$  is the intensity of incident light,  $I$  is the intensity of transmitted light,  $\epsilon$  is the molar absorptivity,  $L$  is the path length (constant), and  $c$  is the concentration [9]. The entire right side of the equation,  $\epsilon Lc$ , is simply the absorption of the light.

In order to use this technique, it is first necessary to measure the transmission peak of light through a solution of h-BN of known concentration, say .2 mg/ml. This peak should be referenced to the pure solvent without h-BN. Then, subsequent measurements should be made using dilutions of the parent material. The raw data that the instrument provides is percent transmission vs. wavelength. This data can easily be converted to absorption vs. energy. With this converted data, the next step is to apply a data fitting approach to create a new plot of absorption vs. concentration. To do so, the absorbance value at each peak should be located for every aliquot. These absorbance values and their corresponding concentrations can be plotted on absorption vs. concentration curves. Ideally, a first order linear fit can be applied for extrapolation purposes. Then, when measuring a suspension of unknown concentration, the absorption value at the peak can be matched on the second order curve to find the associated concentration.

However, for this project, the absorption vs. concentration relationship did not display a linear fit. This could have been due to several reasons, of which cannot be known with complete certainty. One possibility is that the h-BN suspensions may have had stability issues, meaning that sedimenting particles would disrupt the measurements. Another possibility is that the aliquots might not have been accurately measured, which would impair all resulting data. No matter the reason, this method of characterization was discarded for all concentration measurements. As a result, all measurements for this project were done using the previously described evaluation method from Section 3.5.

### **3.7 X-ray Photoelectron Spectroscopy**

For this project, x-ray photoelectron spectroscopy (XPS) was used to examine some of the potential applications of h-BN for radiation sensing. Specifically, this technique was used to determine the changes in the chemical structures of h-BN integrated co-polymer films after being irradiated with thermal neutrons. This characterization technique was chosen because of its ability to determine chemical composition of sample surfaces.

## Chapter 4

### Results and Discussion

#### 4.1 Solvent Comparison

The first comparative study in this report was performed to evaluate the effect of the exfoliation solvent on the h-BN suspensions. As mentioned in prior sections, the 3 solvents that were used in this project were DI water, IPA, and DMF. The latter 2 solvents are polar, organic solvents and are very commonly used for h-BN exfoliation. DI water, on the other hand, is not commonly used because h-BN is hydrophobic. However, due to sonication-assisted hydrolysis of the boron nitride, it becomes an effective solvent for exfoliation [10]. In this project, the 3 of these solvents were compared to evaluate their respective effects on dispersion, agglomeration, and particle size. In order to solely examine the solvent effect, all other exfoliation parameters for this study were held constant. Specifically, the experimental procedure for this solvent comparison involved one suspension of each solvent, all with an initial h-BN concentration of 3 mg/ml. The 3 of these suspensions were made using an h-BN starting powder from Alfa Aesar, with an average starting particle size of 5-10  $\mu\text{m}$ . The suspensions were sonicated for 1 hour at a monitored temperature of 65 °C. Following ultrasonication, the suspensions were centrifuged for 10 minutes at 5,000 rpm. The precipitates of these suspensions were decanted, and the resulting supernatants were kept for characterization.

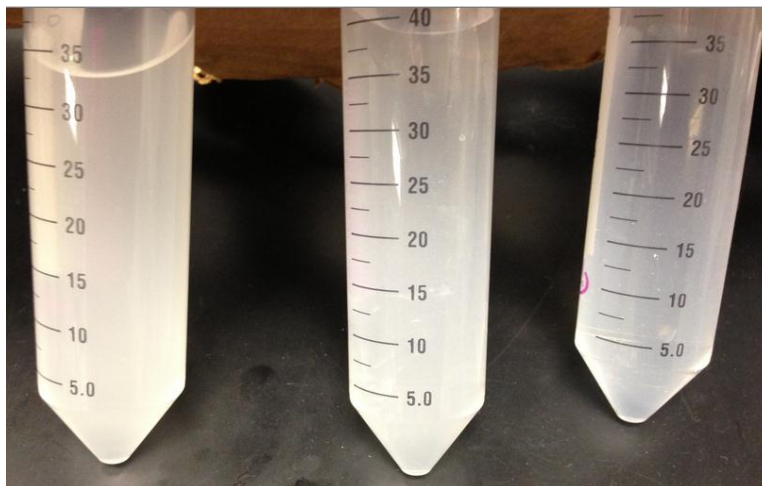


**Figure 4.1:** h-BN supernatants in DMF (left), DI water (middle), and IPA (right).

The supernatants of the suspensions for the solvent comparison are displayed above in Figure 4.1. Though somewhat difficult to tell visually, the concentration yield for DMF and IPA are greater than that of DI water. The calculated concentrations of these suspensions are shown below in Table 4.1, along with the percent yield, which is a measure of the final concentration relative to the initial concentration (3 mg/ml).

<b>Solvent</b>	<b>Measured Concentration</b>	<b>Corrected Concentration</b>	<b>% Yield</b>
<b>DI water</b>	.10 mg/ml	.077 mg/ml	3.86 %
<b>DMF</b>	.32 mg/ml	.147 mg/ml	7.35 %
<b>IPA</b>	.39 mg/ml	.283 mg/ml	14.1 %

**Table 4.1:** Concentration and percent yield for the h-BN suspensions of different exfoliation solvents.

As shown in Table 4.1, the IPA-h-BN solution retained the most boron nitride after centrifugation, while the DI water solution retained the least. Theoretically, this would indicate that IPA is the solvent best suited for h-BN dispersion. However, this conclusion is not confirmed by any other characterization. In fact, by simply looking at the suspensions in Figure 4.1, it appears as if the IPA solution is the least concentrated. Both the DMF and DI water suspensions are milky in appearance, while the IPA suspension looks much clearer. Furthermore, upon closer evaluation in Figure 4.2, it becomes clear that the boron nitride particles are not very well dispersed in the IPA solution, and are simply floating around in the test tube.

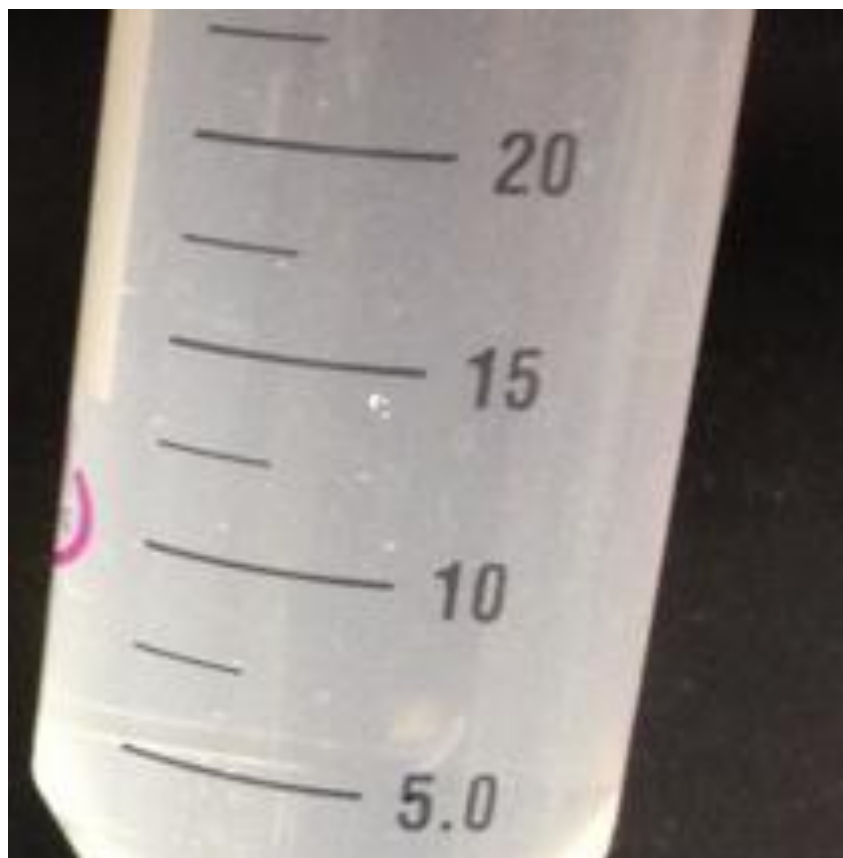


**Figure 4.2:** Zoomed in view of IPA-boron nitride test tube showing floating particles not dispersed in suspension.



Because of this, the solution is still mostly clear in appearance, even though it contains more h-BN by weight in comparison to the other 2 suspensions. Therefore, it is concluded that DMF and DI water are better solvents for h-BN dispersion.

For further characterization, the 3 h-BN suspensions were all deposited onto silicon substrates via drop casting. The optical images of the 3 resultant samples are shown in Figure 4.3.

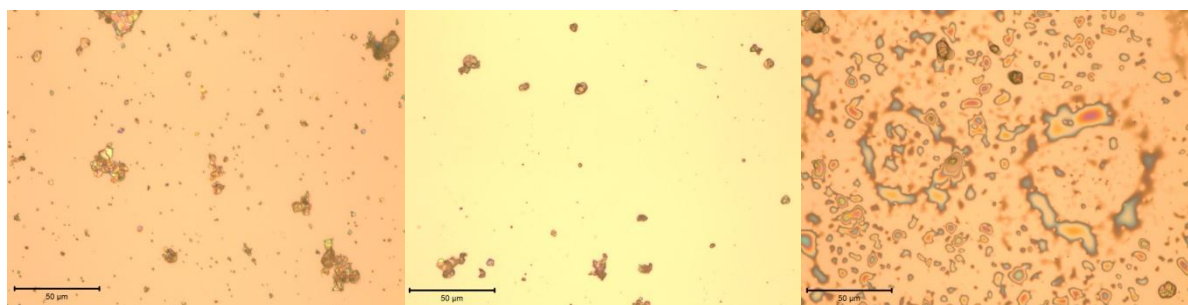


**Figure 4.3:** Optical images of drop casted h-BN suspensions in DI water (left), DMF (middle), and IPA (right). Scale bars = 50  $\mu\text{m}$ .

These images display poor surface coverage of the boron nitride. Interesting to note here, is that the DI water sample has greater surface coverage than the DMF sample. This would not be expected due to the fact that the percent yield for the DMF suspension was almost twice that of the DI water suspension (7.35 % vs. 3.86 %). However, this can be explained from the drop casting procedure. Because of the hydrophobic nature of the silicon substrate, multiple drops of the h-BN-water suspension were necessary to cover the surface. In comparison, just 1 drop was used with the DMF suspension. Thus, more boron nitride was deposited onto the water sample, which explains why the DI water sample has slightly better surface coverage.

For the IPA sample, an unusual occurrence is noticed in Figure 4.3. Even after heating the substrates at 60  $^{\circ}\text{C}$  for 5 minutes to remove excess solvent, there is still a

residual material present on the IPA sample. At this point, it is unknown as to what is causing this interesting phenomenon, and thus more research is required to expand upon this inquiry.

## 4.2 Sonication Impact on h-BN Particle Size

Following the comparative study of the exfoliation solvents, the next goal of this project was to understand the impact that the sonication process had on the h-BN exfoliation. The first relationship that was investigated was the impact of sonication time on the exfoliation of the boron nitride. To explore this, 3 suspensions were again created and sonicated at varying times of 1 hour, 2 hours, and 4 hours. In making sure that outside variables were controlled, DI water was used as the universal solvent. Similarly, the boron nitride starting powder was kept constant throughout, and was the Alfa Aesar 10  $\mu\text{m}$  powder from the previous section. The sonication bath temperature was also closely monitored and held to 65 °C. Table 4.1 lists the 3 suspensions used in this experiment and the corresponding sonication times, as well as the centrifugation information for each suspension.

Suspension Name	h-BN 26 1	h-BN 26 2	h-BN 26 3
Sonication Time	1 hour	2 hours	4 hours
Centrifugation Info.	5,000 rpm/ 30min	5,000 rpm/ 30min	5,000 rpm/ 30min

**Table 4.2:** Sonication and centrifugation information for the h-BN 26 exfoliation run.

The number 26 in the suspension names represents the exfoliation run number. As such, this particular experiment was the twenty-sixth exfoliation procedure done throughout this entire research project. In this specific procedure, the centrifugation process was constant for all 3 h-BN suspensions, as they were all run at 5,000 rpm for 30 minutes. The supernatants of the resultant suspensions after centrifugation were passed through a 5  $\mu\text{m}$  filter paper, and the filtrate was collected for deposition. This was done to limit the range of h-BN particle sizes. The SEM image below in Figure 4.4 displays the drop casted film of h-BN 26 1.

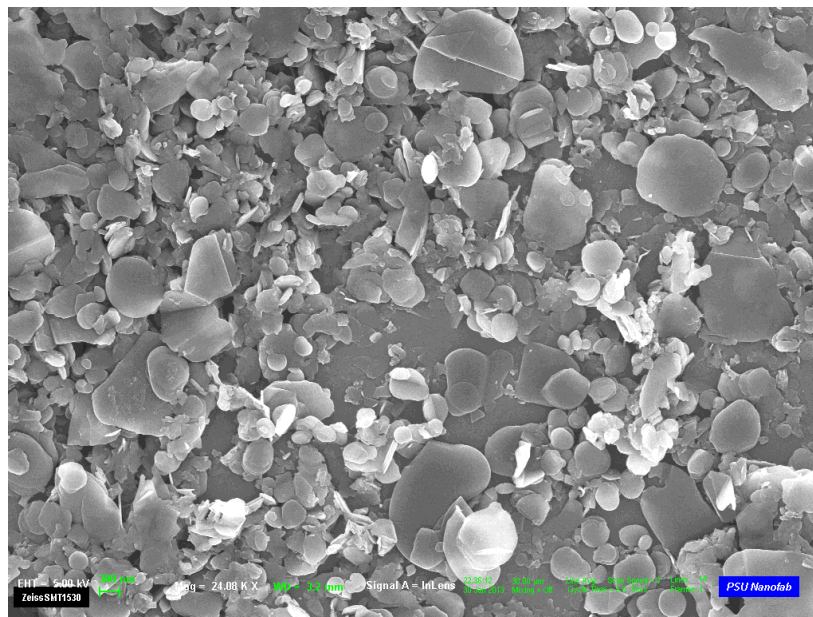
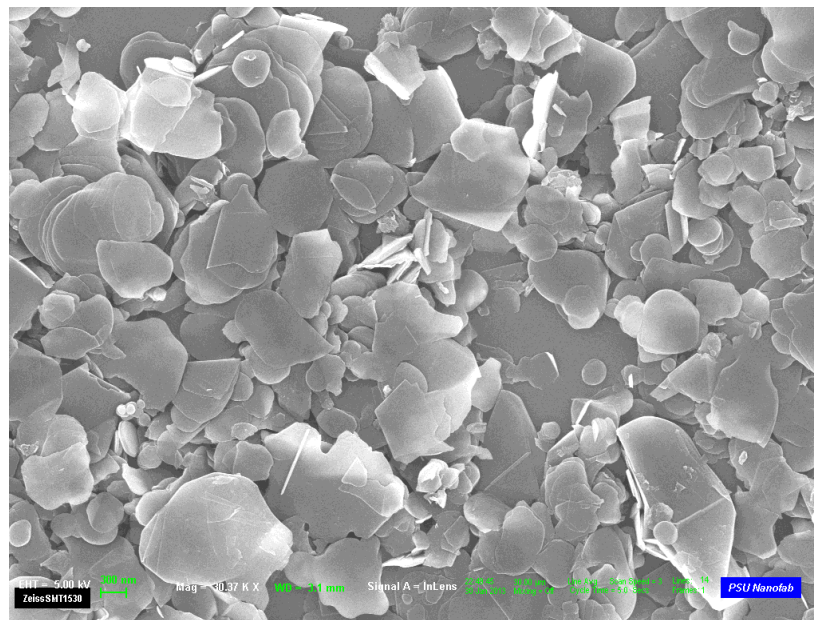


**Figure 4.4:** SEM image of h-BN 26 1 (1 hour sonication). 24 kX magnification. Scale bar = 300 nm.

After 1 hour of sonication, the h-BN particles exhibit varying lateral sizes, with the majority being less than 1  $\mu\text{m}$ . 3 hours later, after a total sonication time of 4 hours, there appears to be a lack of disparity in the h-BN particle's lateral sizes in comparison to the 1 hour sample.



By visual inspection, it appears as if the range in particle size is similar in the samples from the 1 hour and 4 hour sonication. As a matter of fact, one might even say that the 4 hour sample has h-BN particles that are larger than the 1 hour sample. However, due to the small scan area in SEM, it is difficult to get an accurate size distribution for the entire sample. Therefore, this is not a very accurate measure of comparing the two suspensions. Instead, comparisons made with dynamic light scattering are more practical because of this technique's ability to provide full size distribution relations.

Although this presents a caveat with using SEM for particle size comparison, it is still effective in providing a visual description of the effect of sonication time on h-BN particle size. From a visual comparison standpoint, it appears that the increased sonication time resulted in h-BN particles with sharper edges, and possibly smaller thicknesses. However, there are more appropriate characterization techniques to determine particle thickness, and so AFM was used to further explore this hypothesis. This will be expanded upon in later sections.

In continuing with the size comparison of this sonication parameter study, DLS measurements were taken for each of the 3 suspensions.

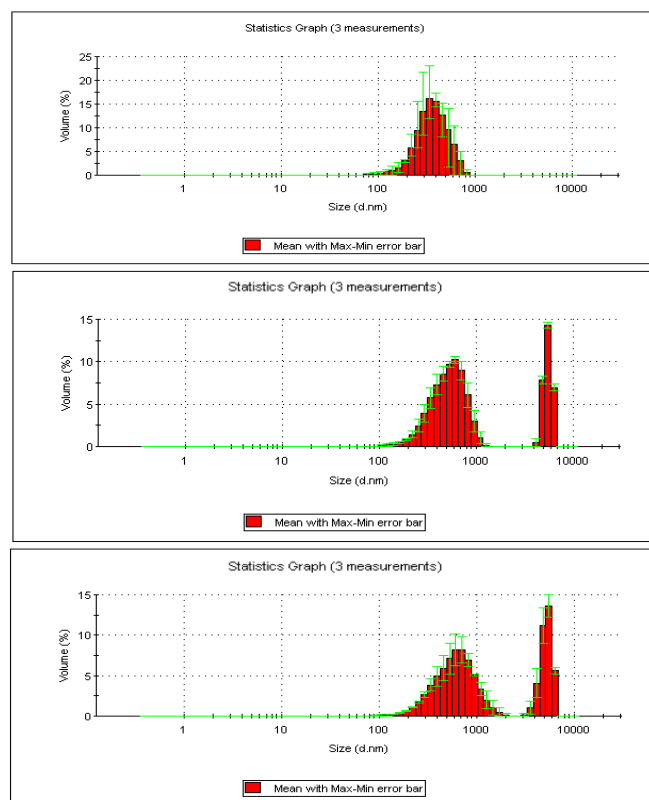


**Figure 4.6:** DLS measurements for h-BN 26 1 (top), h-BN 26 2 (middle), and h-BN 26 3 (bottom). Each suspension was measured 3 times and averaged to create these size distributions by volume percent.

Figure 4.6 illustrates an interesting occurrence with the suspensions that were sonicated for more than just 1 hour. Multiple peaks in the size distribution charts are present in both the 2-hour and 4-hour suspensions. For h-BN 26 2, the first peak is centered at 428 nm, while the second peak is centered at 5.6  $\mu\text{m}$ . For h-BN 26 3, the first and second peaks are centered at 488 nm and 5.3  $\mu\text{m}$ , respectively. When this characterization technique provides multiple peaks, it is an indication that the h-BN particles are agglomerating in solution. When there is agglomeration present, the DLS technique is unable to distinguish between individual h-BN particles. Because of this, congregated particles are characterized as individuals, which results in peaks that are beyond 1  $\mu\text{m}$ . Here, this data suggests that longer sonication times have an effect on particle agglomeration. To further explore this phenomenon, sonication times were increased even further.

### **4.3 Sonication Time and Particle Agglomeration**

To initiate this inquiry, a new h-BN suspension was exfoliated in the same fashion as the previous 3, only this time at 12 hours. The results of this experiment are shown below in the size distribution chart from DLS in Figure 4.7.

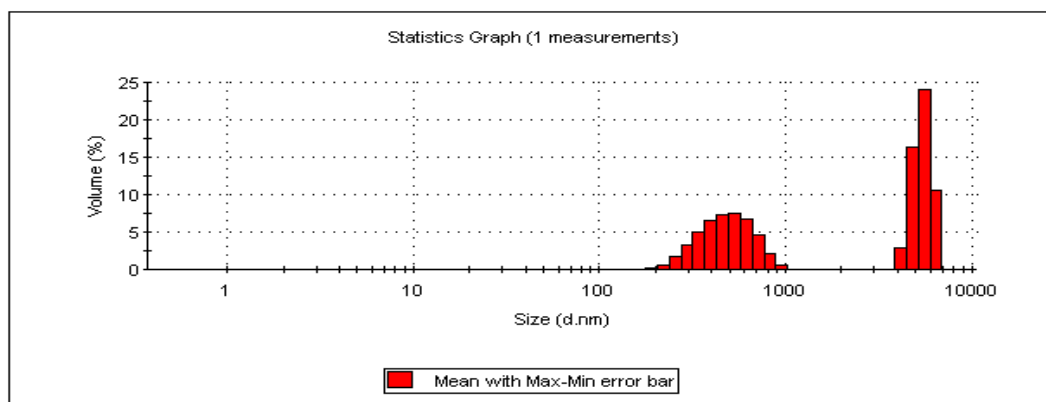


**Figure 4.7:** DLS measurement for the h-BN suspension that was sonicated for 12 hours. Only 1 measurement was used for the making of this distribution.

As shown in this figure, the relationship between the sonication time and particle agglomeration is again evident. Here, there is an even greater percentage of the h-BN particles that are present in the second peak. Specifically, the particles in this second peak account for 53.7 % of all h-BN particles in the suspension. Thus, it can be concluded that sonication does in fact promote particle agglomeration in suspension. Furthermore, this also confirms that longer sonication times account for greater amounts of agglomeration. To support this finding, SEM imaging also shows the increase in particle agglomeration of this 12-hour sonicated suspension. Figure 4.8 below displays a visual illustration of this effect. Here, the agglomeration of the h-BN particles is exceptionally noticeable, especially in the right side of the image.



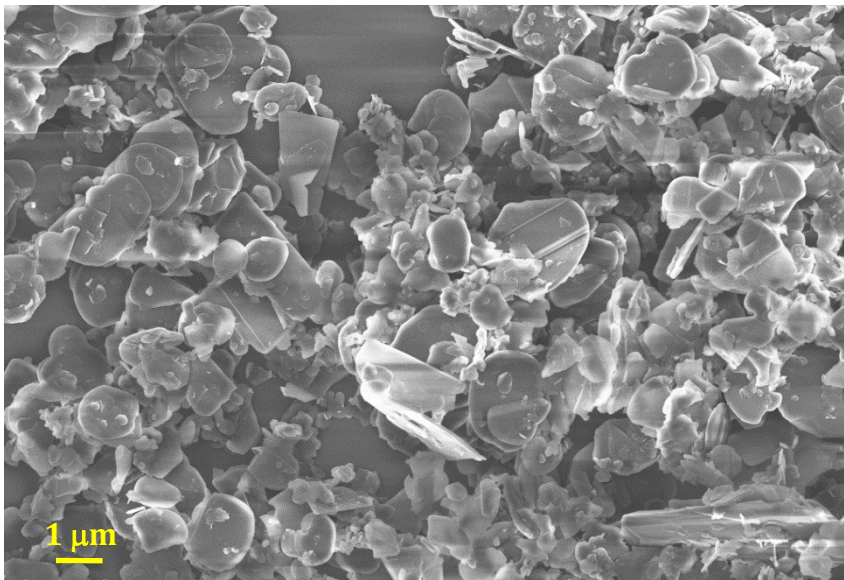


**Figure 4.8:** SEM image of the 12-hour sonicated h-BN suspension drop casted onto silicon.

At this point, the reasoning behind this occurrence is unclear. However, an important relation to note is that as sonication time increases, so does the concentration yield of the suspension following the removal of the precipitate. Therefore, this presents speculation as to whether or not the concentration of the boron nitride is ultimately causing the increase in particle agglomeration.

#### **4.4 h-BN Concentration vs. Particle Agglomeration**

As previously mentioned, it is apparent that sonication has a direct effect on the amount of final h-BN retained in suspension after precipitate removal. From the previous sonication study, there is a noticeably visual difference in the appearance of the 3 suspensions, due to the dissimilar concentrations of boron nitride in each. Figure 4.9



below illustrates this concept, as it is evident that the suspension to the right (4-hour sonication) is much more concentrated than either of the other 2 suspensions.

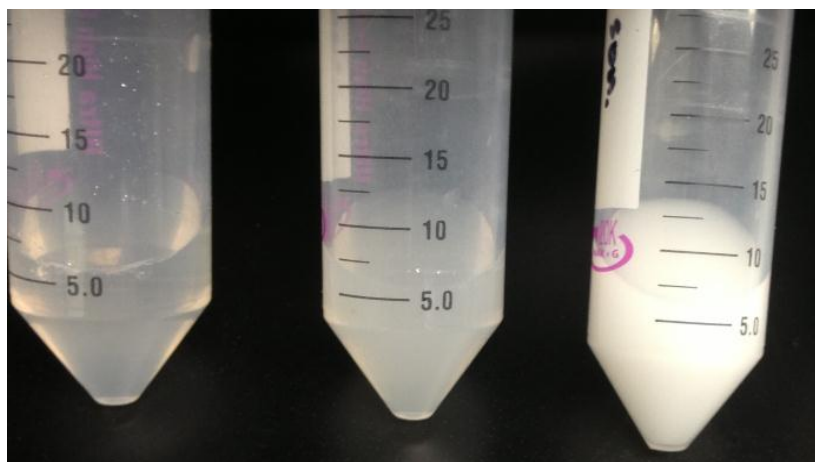


**Figure 4.9:** Image of h-BN 26 1 (left), h-BN 26 2 (middle), and h-BN 26 3 (right).

In theory, this is expected, as the sonication process aids in dispersing the boron nitride in the solvent. For DI water, the significance of this effect is even greater due to the fact that boron nitride is commonly known to be hydrophobic in nature. Thus, sonication-assisted hydrolysis of the h-BN is directly related to the concentration of the suspension. Table 4.3 quantitatively displays the relationship between the sonication time and the amount of boron nitride retained in suspension.

<b>Sonication Time</b>	<b>Measured Concentration</b>	<b>Corrected Concentration</b>	<b>% Yield</b>
<b>1 hour</b>	.114 mg/ml	.09 mg/ml	3.0 %
<b>2 hours</b>	.279 mg/ml	.24 mg/ml	8.0 %
<b>4 hours</b>	.972 mg/ml	.87 mg/ml	<b>29.0 %</b>

**Table 4.3:** Concentration and percent yield for the h-BN suspensions of different sonication times.

Once again, the percent yield is the ratio of the final concentration (corrected) with respect to the initial concentration (3 mg/ml). As shown, the h-BN suspension that was sonicated for 4 hours retained more than 9 times the amount of the 1 hour suspension and more than 3 times the amount of the 2 hour suspension.

To determine whether this relation had an effect on the agglomeration phenomenon, a concentration study was performed using DLS. In this study, h-BN 26 2 and h-BN 26 3 were diluted to match the concentration of h-BN 26 1. Therefore, each of the 3 h-BN suspensions were equal in concentration (.09 mg/ml), but still had experienced different sonication times.

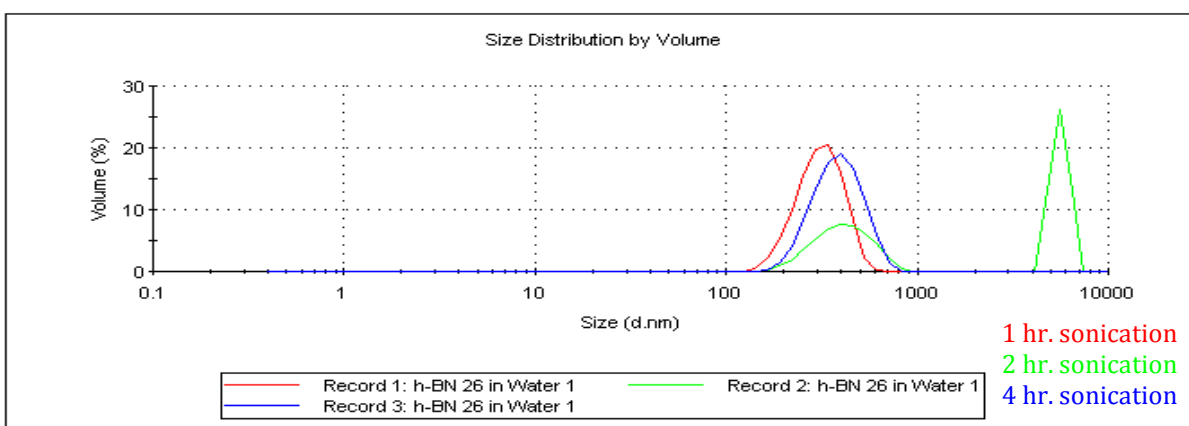


**Figure 4.10:** DLS size distribution chart by intensity percent for h-BN 26 1 (red), h-BN 26 2 (green), and h-BN 26 3 (blue). All suspensions had equal concentrations of .09 mg/ml.

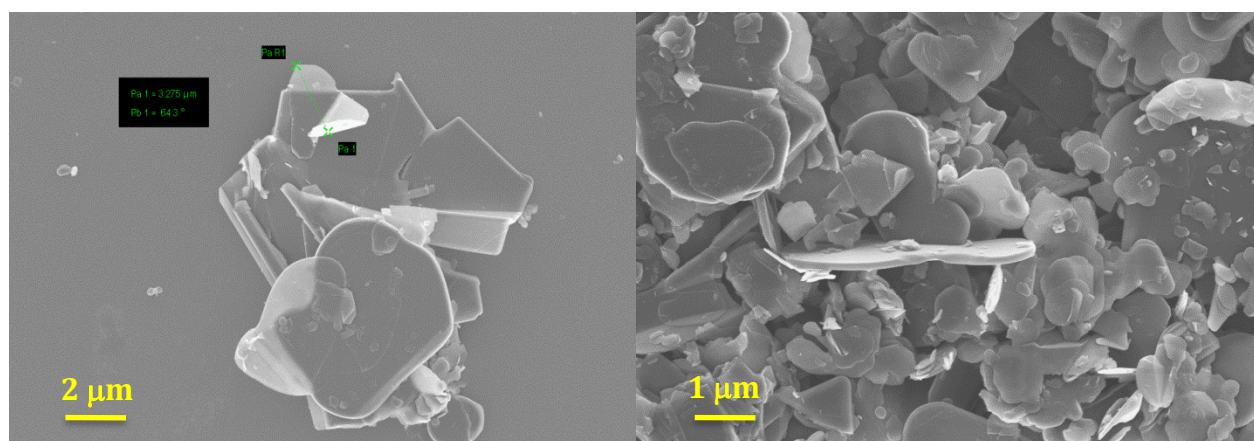
In Figure 4.10, the green representation of h-BN 26 2, which was tailored to be equal in concentration to h-BN 26 1, once again exhibits 2 peaks. However, the blue representation of h-BN 26 3 does not show this second peak. These results are somewhat contradictory, as the second peak would be expected to be shown in the 4 hour sonicated

suspension before the 2 hour suspension. Thus, these results are inconclusive, and it remains to be unknown as to whether or not concentration is a factor in the agglomeration of h-BN particles. Furthermore, it is still unclear as to why ultrasonication has a direct impact on particle agglomeration, and so further research is required.

## 4.5 Solvent Impact on Particle Agglomeration

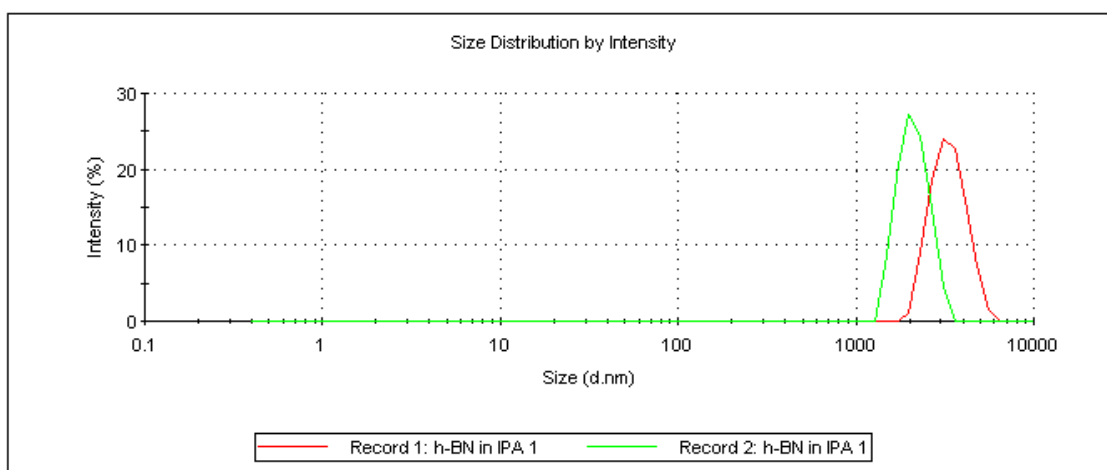
In continuing with the agglomeration relationships with exfoliation parameters, the next study in this report evaluated the impact of the solvent on the extent of h-BN agglomeration. For this particular study, a continuation was made upon the previous sonication time experiment, in which the h-BN suspension was sonicated for 12 hours. Previously, DI water was used as the solvent for this 12-hour sonication process. However, to evaluate the effect of solvent on particle agglomeration, 2 additional suspensions were exfoliated (1 in IPA, 1 in DMF). For consistency measures, these suspensions were exfoliated identically to the previous 12 hour-exfoliation run, with the only difference being the exfoliation solvent. Additionally, these suspensions were tailored to be equal in concentration, due to the fact that the concentration relation with agglomeration was previously ruled inconclusive.

Figure 4.11, below, displays a side-by-side comparison of drop casted samples from the suspensions that were sonicated for 12 hours. The SEM image to the left is from h-BN exfoliated in DMF, while the image to the right is h-BN exfoliated in IPA.



**Figure 4.11:** Comparison of SEM images from drop casted samples from h-BN suspensions that were sonicated for 12 hours. Displayed to the left is the h-BN exfoliated in DMF, while the right is the h-BN exfoliated in IPA.

As previously mentioned, the suspensions used in these samples were equal in concentration. Visually, there is a distinct difference in the coverage of the h-BN particles. The boron nitride particles from the DMF suspension are much more isolated and dispersed across the substrate. In comparison, the particles from the IPA suspension are all extremely agglomerated. From this, it can be concluded that DMF is the best solvent for h-BN dispersion, due to the fact that deposition of h-BN suspensions in DMF leads to greater isolation of particles. As for IPA, the agglomeration of the h-BN particles was further explored using dynamic light scattering. Figure 4.12, below, displays the size distribution chart for 2 consecutive runs of the h-BN suspension in IPA. As shown, 100 % of the particles are characterized to be beyond 1  $\mu\text{m}$  in size. However, by visual inspection of the IPA image in Figure 4.11, this is not actually the case.



**Figure 4.12:** DLS size distribution chart by intensity percent for h-BN suspension sonicated for 12 hours in IPA. The red and green records indicate successive runs of the same suspension.

What this means is that the DLS instrument is unable to differentiate between individual particles because of the large amounts of particle agglomeration. This is an indication that IPA promotes agglomeration in a similar way that ultrasonication does.

## 4.6 Centrifugation and h-BN Particle Size

Following the evaluation of ultrasonication and solvent relations on boron nitride exfoliation, the next study focused on the relationship between centrifugation and particle size. As with each of the previous studies, all other exfoliation parameters were held constant during this experiment. The boron nitride powder used was the 5-10  $\mu\text{m}$  powder from Alfa Aesar, and the suspensions were exfoliated in DI water. Although it was previously concluded that DMF is the best solvent for h-BN dispersion during exfoliation, DI water was generally chosen as the universal solvent for each of the experiments. This is due to several reasons, including water's ease of use and safety, and also because of limitations in the abundance of DMF. For this study, these h-BN-DI

water suspensions were sonicated for 1 hour at a controlled temperature of 65 °C. They were then centrifuged at various angular rates and times. The specific centrifugation rates and times are listed below in Table 4.4. Once again, the number 27 in the suspension name refers to the exfoliation run number.

<b>h-BN Suspension</b>	<b>Centrifugation Rate/Time</b>
h-BN 27 1	2,000 rpm/ 1 hour
h-BN 27 2	8,000 rpm/ 1 hour
h-BN 27 3	10,000 rpm/ 5 hours

**Table 4.4:** Centrifugation information for h-BN 27 exfoliation suspensions 1, 2, and 3.

Following centrifugation, the 3 h-BN suspensions were drop casted onto silicon substrates for characterization. A comparison of the first 2 suspensions was done initially, and the results are shown through SEM imaging in Figure 4.13 below.

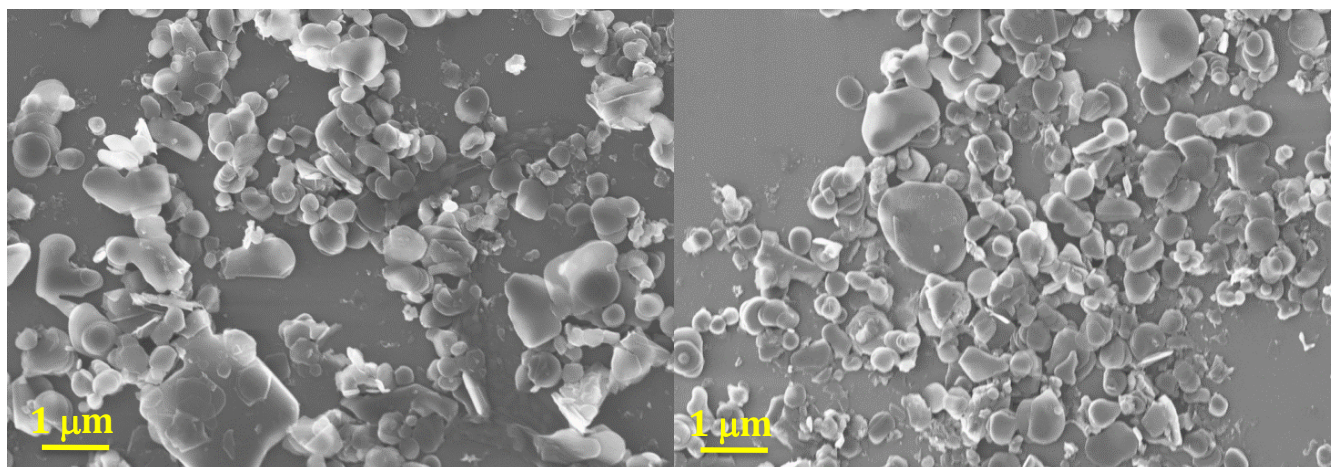


**Figure 4.13:** SEM comparison of h-BN 27 1 (left) and h-BN 27 2 (right).

From the images in Figure 4.13, it is difficult to distinguish between any differences in the overall size distribution from the 2 samples. By visual inspection, it can potentially be concluded that the particles on the right (8,000 rpm) are slightly smaller



than those on the left (2,000 rpm). However, without qualitative data, it is difficult to tell. It is fairly evident though, that the particle sizes are within the same general range, with the majority of them being 1  $\mu\text{m}$  or less in lateral size. This concludes that there is no significant disparity among the 2 samples, which differed by a factor of 4 in angular centrifugation speed.

Next, to determine whether or not drastic changes in centrifugation result in smaller particle sizes, these suspensions were compared to h-BN 27 3.

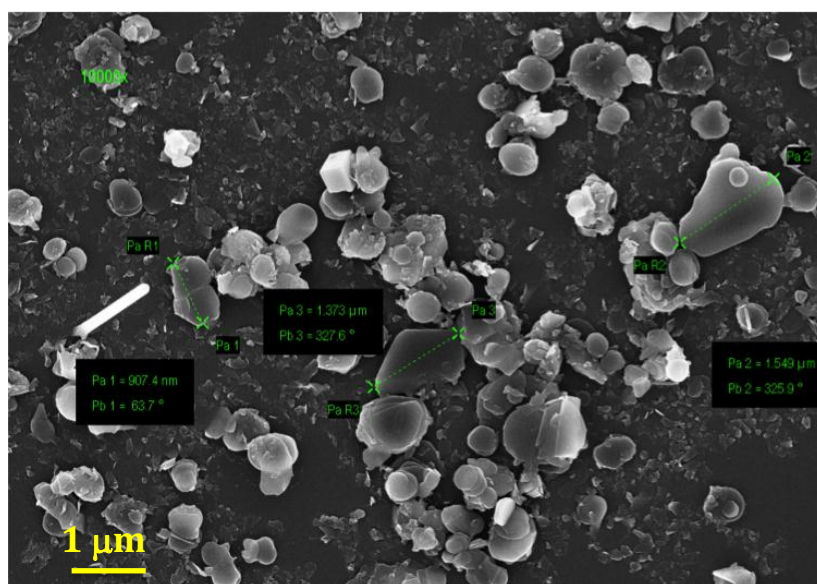


**Figure 4.14:** SEM image of h-BN 27 3. Centrifuged for 5 hours at 10,000 rpm.

Figure 4.14 illustrates the particle sizes of the boron nitride after 5 hours of centrifugation at 10,000 rpm. While there are still several particles on the order of 1  $\mu\text{m}$ , it is apparent that the particle size range has expanded. This particular image shows several areas on the substrate which are highly populated with boron nitride nanoparticles. From this data, it can be concluded that drastic changes in centrifugation do in fact result in noticeable changes to the boron nitride particle size. However, to

confirm these findings through further characterization, AFM was used to examine the heights of the h-BN particles, as opposed to just the lateral sizes.

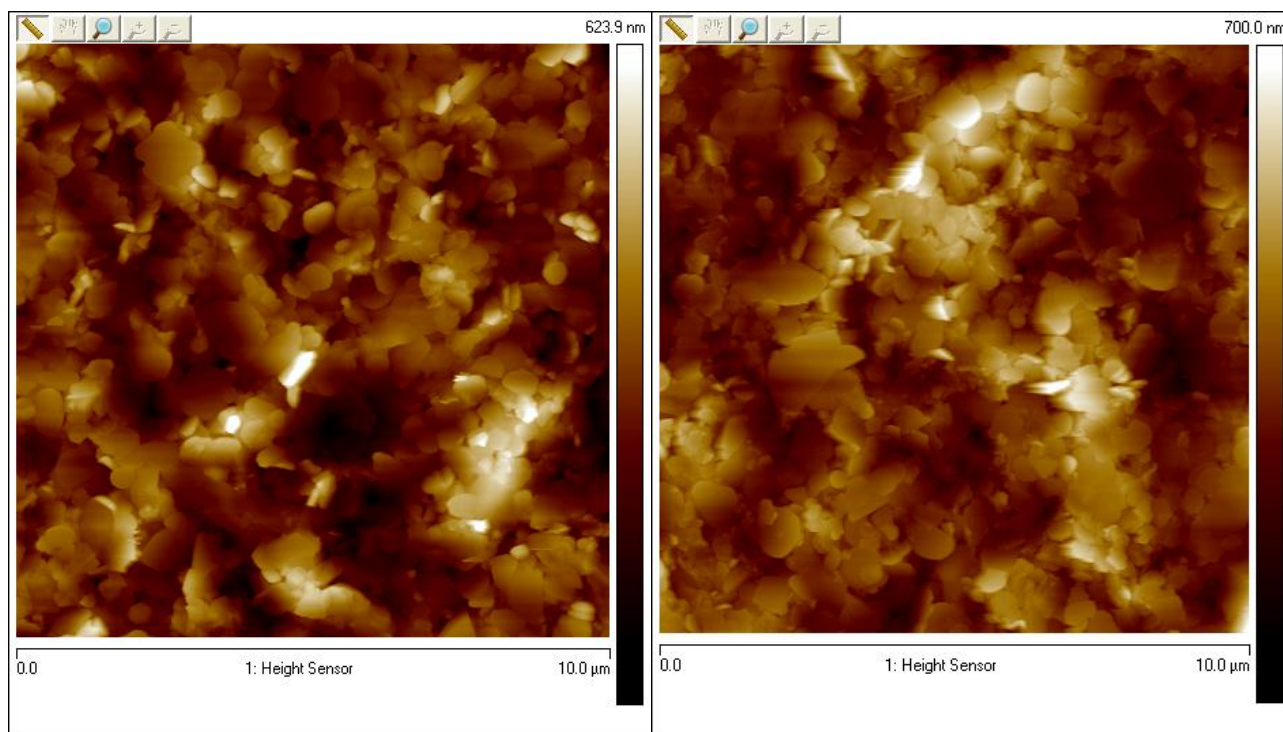


**Figure 4.15:** AFM height profile images of h-BN 27 1 (left) and h-BN 27 2 (right).

Figure 4.15 illustrates the height profiles of boron nitride particles from h-BN 27 1 and h-BN 27 2. Similar to the SEM images in Figure 4.13, the particles here display comparable and non-differentiable results. When looking at the step heights from 9  $\mu\text{m}$  sections of these samples, the relative heights of the boron nitride particles can be seen.

This is illustrated in Figure 4.16.

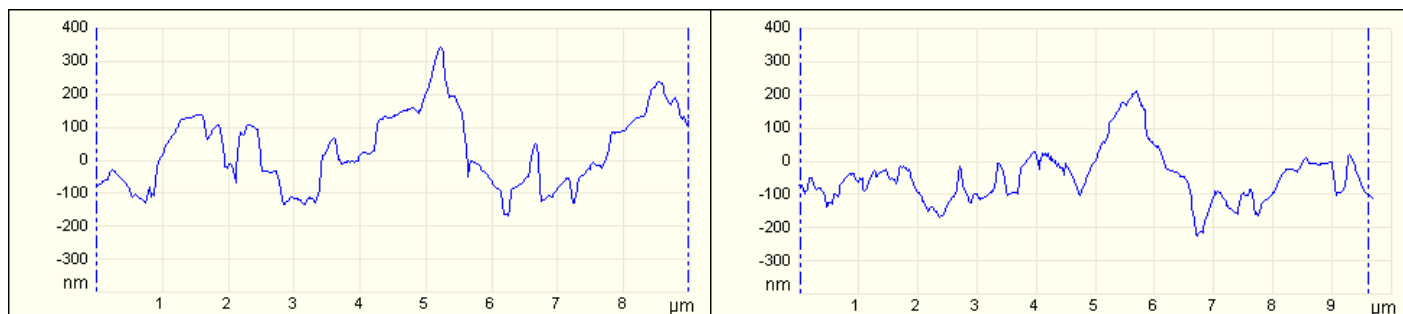


**Figure 4.16:** AFM step height display of h-BN 27 1 (left) and h-BN 27 2 (right).



From this comparison, there is a slight decrease in the heights of the particles from the sample that was centrifuged at a higher rate. However, this change is almost negligible. Once again though, when looking at a sample that was centrifuged for much longer, and at a higher angular speed, there is a noticeable difference in the h-BN particle size. Figure 4.17, below, displays the significant decrease in h-BN particle heights after being centrifuged for 5 hours at 10,000 rpm (h-BN 27 3).

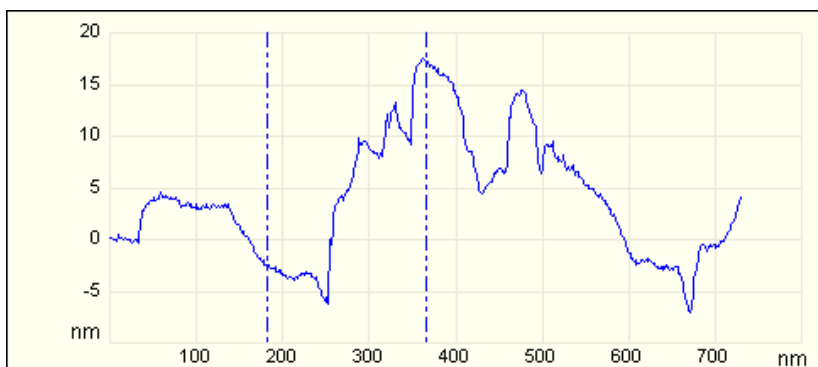


**Figure 4.17:** AFM step height display of h-BN 27 3.

Important to note here, is that the AMF scan for this sample was taken in an area with a high population of h-BN nanoparticles, even though the sample did include much larger particles as well. These results are consistent with what was found in the SEM imaging of the same samples. As a result, it can be concluded that drastic changes in centrifugation do result in h-BN particles with both decreased lateral sizes and heights.

## 4.7 Boron Nitride Starting Powder Evaluation

Up until this point, the boron nitride starting powder was held constant. For all previous experiments, the 5-10  $\mu\text{m}$  powder from Alfa Aesar was used during exfoliation. Initially, one of the goals of this project was to extract large, single-flake particles of boron nitride. For this reason, the Alfa Aesar powder was used, as it contains relatively

large h-BN particles compared to powders from other companies. However, as the goals of this project evolved, the comparison of different starting powders became a new avenue to explore. As a result, a second h-BN powder was introduced into the project and compared with the 5-10  $\mu\text{m}$  powder.

The second h-BN starting powder was purchased from MK Impex Corp, and had an average particle size of 70 nm. To compare the 2 powders, a general exfoliation procedure was performed. The 2 powders were first dispersed in DI water with an initial concentration of 3 mg/ml. The suspensions were then sonicated for 1 hour at 65 °C and centrifuged for 10 minutes at 5,000 rpm. The precipitates of the 2 suspensions were decanted, and the supernatants were collected for characterization. From a visual comparison standpoint, the 70 nm starting powder suspension has a much higher concentration after centrifugation. This can easily be seen in Figure 4.18 below.

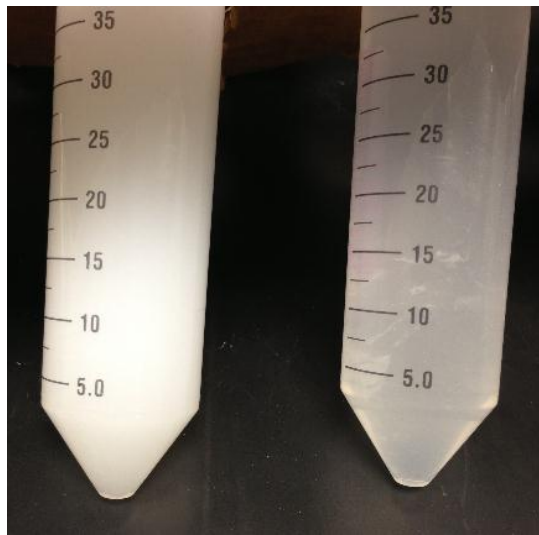


**Figure 4.18:** Image comparison of starting powders after precipitate removal. 70 nm suspension (left) and 10  $\mu\text{m}$  suspension (right).

Furthermore, to quantify the visual findings from this figure, the concentrations of these suspensions were calculated, and are shown below.

Starting Powder	Measured Concentration	Corrected Concentration	% Yield
70 nm	.40 mg/ml	.35 mg/ml	17.5 %
5-10 $\mu\text{m}$	.10 mg/ml	.077 mg/ml	3.86 %

**Table 4.5:** Concentration and percent yield for the h-BN suspensions of different starting powders.

Table 4.5 displays both the concentration and percent yield for the 2 h-BN suspensions. Again, the percent yield is a measure of the final concentration in relation to the initial concentration (3 mg/ml). As shown, the 70 nm h-BN suspension had a much greater % yield, as 17.5 % of the original boron nitride remained in suspension after centrifugation. Compared to the other starting powder, this is an order of 4.5 times greater. This concludes that the 70 nm starting powder is better suited for dispersion in DI water.

In continuing with this comparison, the suspensions were drop casted onto silicon substrates for size measurements. Using optical microscopy, the percent yield findings are further confirmed. The drop casting of the 70 nm h-BN suspension created what appears to be a uniform thin film with high surface coverage. The 5-10  $\mu\text{m}$  suspension, on the other hand, created a sample with much more particle isolation and exceptionally less surface coverage. This behavior is illustrated below in Figure 4.19.

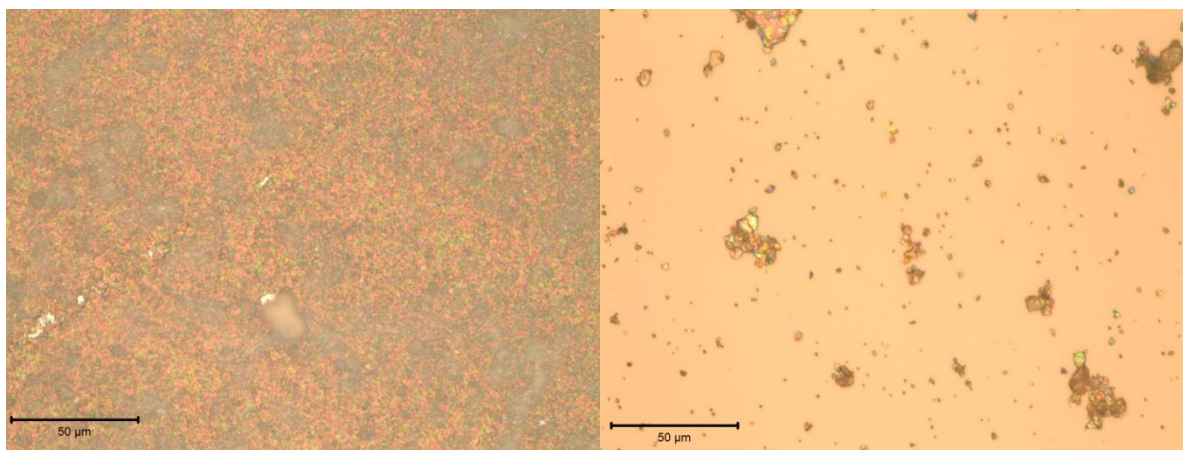


**Figure 4.19:** Drop casted samples from h-BN suspensions with 70 nm powder (left), and 5-10 μm powder (right). Scale bars = 50 μm.

These optical images do confirm the fact that the 70 nm powder is better suited for dispersion in DI water during chemical exfoliation.

## Chapter 5

### Applications and Future Work

#### 5.1 Radiation Sensing

While the potential uses for h-BN are vast and relatively unexplored to date, there is one application that this report focused on. That is, the use of boron nitride as a radiation sensing element. The concept of using boron nitride for radiation sensing begins with the integration of the h-BN into a co-polymer film. For this project, poly[(vinylidene fluoride-co-trifluoroethylene] (PVDF-TrFe) was chosen as the co-polymer film. The reasoning behind this is that PVDF-TrFe is sensitive to thermal neutrons. Therefore, when introduced to neutron radiation, the electronic properties of this material change. The changes in this film can thus be traced back to sources of radiation.

For the integration of h-BN into the co-polymer films, it was first necessary to make sure that the h-BN suspensions were high enough in concentration (around 1.0 mg/ml). This is due to the fact that it is easier to reach a desired viscosity when the concentration of h-BN is higher. Once the h-BN suspension was created, the polymer powder was mixed into the h-BN suspension. For general measurements, the weight of the polymer was typically around one-sixth that of the solvent. The resultant suspension was then stirred for 2 hours at a controlled temperature of 60 °C. Then, once the desired viscosity was reached, the mixture was placed under vacuum for about 10 minutes to remove all air bubbles. At this point, the mixed solution was poured onto a large glass plate and spread out using a casting knife. With this knife, it was possible to control the ultimate thickness of the film. Once the solution was spread across the plate to a desired

thickness, it was left to dry under vacuum for approximately 3 hours. After the drying period, the films were removed from the plate, and ready for characterization.

For characterization, XPS was used to evaluate chemical changes in the film after being exposed to radiation. When performing this characterization on the h-BN integrated films of various h-BN concentrations, there was one consistent problem throughout. The problem was that the XPS did not detect any boron or nitrogen at all in any of the samples. Although the h-BN concentrations within the co-polymer films were relatively low (from .1 weight % to 8.5 weight %), the boron nitride particles were still visibly present in the films. The absence of boron and nitrogen detection is most likely due to the fact that XPS is a surface sensitive characterization technique that only accurately measures the top 10 nm of the sample. Because of this, it was difficult to evaluate the effect of the h-BN concentration in the film on the chemical changes within the PVDF-TrFe.

However, XPS data from the pure PVDF-TrFe film shows interesting results that are intriguing and hopeful.

	Start	t=11hrs	t=23hrs	$\Delta\%$
Si 2p (%)	3.5	3.5	3.6	
C 1s (%)	78.8	79.6	79.8	1.0
O 1s (%)	11.6	11.7	12.2	0.6
F 1s (%)	6.1	5.1	4.3	1.8

**Figure 5.1:** Percent composition of silicon 2p, carbon 1s, oxygen 1s, and fluorine 1s over 23 hour period of alpha radiation from Po-210 alpha generator.

In Figure 5.1, above, there are slight changes in the compositions of carbon, oxygen, and fluorine after being exposed to alpha particles for 23 hours. This is significant because when h-BN integrated films are exposed to neutron radiation, the boron-10 isotope generates an alpha particle. The generation of alpha particles results in a change of energy, which in turn causes electronic properties in the PVDF-TrFe to change. Again, this is due to the fact that PVDF-TrFe is a neutron sensitive material. Therefore, the data in Figure 5.1 simulates some of the chemical changes caused by the existence of alpha particles. However, in this case, the alpha particles were generated from a Po-210 source, instead of the B-10 isotope. The fact that there are noticeable changes in the elemental composition, even though they are small, is encouraging. In moving forward, the goal would be to increase the boron nitride concentration in the co-polymer film, such that boron and nitrogen can be detected by XPS characterization. Additionally, this would consequently increase the thermal sensitivity of the film, which would result in more effective sensing.

## **5.2 Acid Intercalant Exfoliation**

As far as other future work surrounding h-BN exfoliation is concerned, there are other means of exfoliation that were not discussed thus far in this project. This includes the exfoliation of boron nitride in acids. For example, previous investigations have used phosphoric, sulfuric, and even hydrochloric acid for exfoliation solvents. By introducing h-BN to these acids, the exfoliation process can potentially be assisted by the intercalation of the acidic ions between the h-BN sheets. However, at the same time, the strong nature of the acids can have a destructing effect on the h-BN sheets, and can

potentially damage them. Therefore, when exfoliating h-BN in acids, it is necessary to limit the time of the sonication period, as this is when the damage can result.

During this specific project, a suspension of h-BN that was exfoliated in phosphoric acid was gathered from another group for characterization purposes.

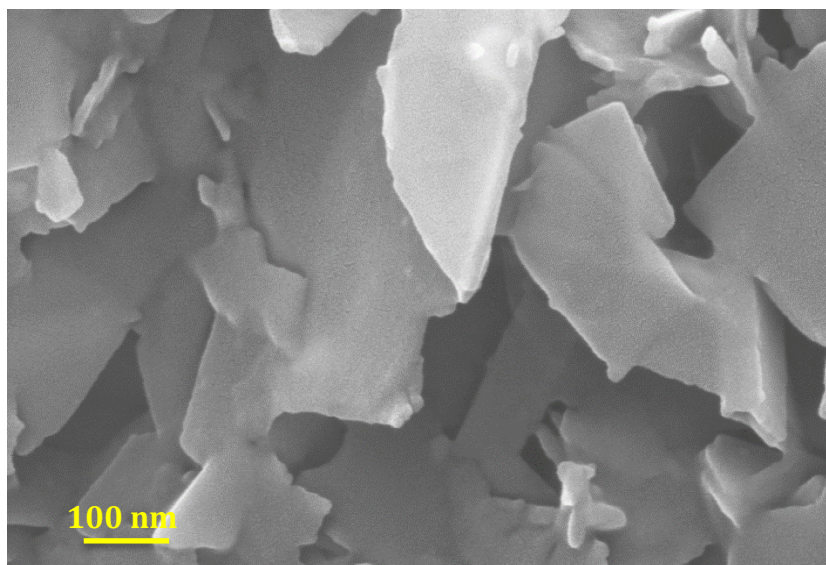


**Figure 5.2:** SEM image of h-BN exfoliated in phosphoric acid.

Figure 5.2, above, displays the resultant boron nitride flakes after exfoliation in phosphoric acid. From this image, it is apparent that the h-BN edges are a lot sharper than what had previously been seen in this report. Additionally, there is a lot of folding of the h-BN edges that allows for thickness measurements. Though it is difficult to accurately measure these edges using SEM, especially at such a small scale, it can be estimated that these flakes are less than 10 layers thick. Using AFM, this estimation can be quantified. Shown below in Figure 5.3 is the step height profile of an h-BN flake from the acid exfoliated suspension. The data here displays a height of about 23 nm, which is most likely equivalent to tens of layers.



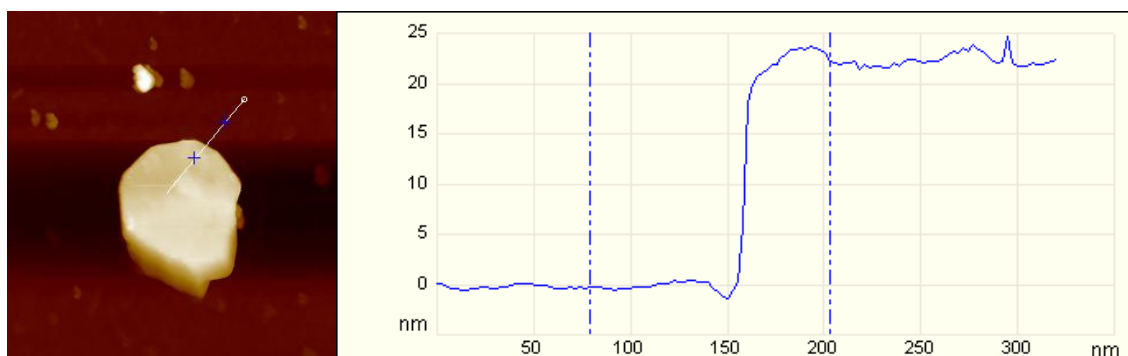


**Figure 5.3:** AFM image of h-BN flake from acid exfoliation (left) and corresponding step height (right).

However, from the image to the left in Figure 5.3, it seems as if there is actually a stacking of at least 2 h-BN flakes. Therefore, this height measurement is not necessarily accurate, and so it can be predicted that the true height of a single flake is actually less than 23 nm.

This method of exfoliation provides a new avenue for extracting few-layered h-BN sheets. With continued research in this area, it may be possible to exfoliate monolayered h-BN species without needing to go to extreme levels of sonication and centrifugation.

## Chapter 6

### Conclusions

This report was able to successfully expand upon previous h-BN investigations and provide new relationships that are important in understanding the chemical exfoliation process of h-BN. First, during deposition, it was noted that drop casting techniques provide much greater surface coverage compared to spin coating. However, in doing so, the h-BN particles become much more agglomerated. In thin film preparation, it was concluded that h-BN concentrations of at least .40 mg/ml were necessary in order to achieve sufficient surface coverage using spin coating.

In regards to methods of characterization, several tests were performed to determine which techniques would be accurate in measuring the sizes of h-BN particles. While optical profilometry was desired for its capability to provide large, fast scans, it was not deemed a practical measuring technique due to several issues. The main problem was that there is no way to accurately distinguish between individual particles and agglomerated particles due to the low lateral resolution. This made it difficult to extract accurate data for evaluation h-BN particle sizes. The next characterization method, dynamic light scattering, was compared to both SEM and AFM in an accuracy study. It was concluded that this method is capable of providing accurate size distribution data for h-BN particles in suspension, even though the particles are not necessarily spherical. Additionally, it was also concluded that this method of characterization has precision, as it provided repeatable data on consecutive runs.

As far as concentration evaluation of h-BN suspensions, it was found that UV-Vis is not an accurate technique due to the non-linear relationship between absorption and

concentration. Instead, this report used a different evaluation method. In this “evaporation” method with the OHAUS microbalance, it was noted that for each of the 3 exfoliation solvents (DI water, DMF, IPA), there was an overestimation in the concentration measurement due to a residual effect. Thus, this was effectively accounted for by determining the linear relationship between the measured concentration of the suspension and the true concentration.

During the numerous experimental studies on h-BN in this project, there were several conclusions relating the exfoliation parameters to the characteristics of the final h-BN. First, in the solvent comparison, even though IPA was able to retain the most boron nitride after precipitate removal, it was actually the worst solvent for h-BN dispersion. Additionally, it was found that IPA promotes h-BN particle agglomeration in suspension. On the other hand, DMF was the best of the 3 solvents in dispersing the boron nitride.

Next, in terms of the effect of sonication on h-BN exfoliation, it was concluded that sonication times have a direct effect on particle agglomeration. While it was inconclusive as to whether or not the h-BN concentration is the cause of this agglomeration relation, it was apparent that as sonication times increase, so does particle agglomeration.

Following the sonication studies, the effect of centrifugation on h-BN particle size was examined. Conclusively, it is understood that there are generally negligible changes in h-BN lateral sizes and heights, unless there is a drastic change in the centrifugation (rate and time).

As for forthcoming work, there is still a lot that needs to be understood about this material. This project briefly touched on a few areas that can potentially be new avenues

for future exploration. One of these areas involves the effect that boron nitride starting powder has on the chemical exfoliation. This report only included a comparison of 2 different powders. However, it was concluded that the 70 nm boron nitride powder was better suited for h-BN dispersion, as compared to the 5-10  $\mu\text{m}$  powder.

As for other future work, there is great work to be done in integrating boron nitride into co-polymer films for radiation sensing. This project was able to show slight changes in elemental composition of a co-polymer film after exposure to alpha particles. In a similar sense, there is still plenty of work to do in enhancing exfoliation procedures for monolayer h-BN extraction. This report briefly touched on an acid intercalation method, in which h-BN flakes of around 10 layers were exfoliated.

Overall, this project was successful in developing an understanding of h-BN relations during chemical exfoliation. From here, there are ample opportunities for future work in this area, for h-BN applications are only beginning to be understood.

## Bibliography

- [1] Lin, Y., Williams, T., & Connell, J. (2009, November 9). *Soluble, Exfoliated Hexagonal Boron Nitride Nanosheets*. The Journal of Physical Chemistry Letters.
- [2] Lian, G., Zhang, X., Tan, M., Zhang, S., Cui, D., & Wang, Q. (2011, April 20). *Facile synthesis of 3D boron nitride nanoflowers composed of vertically aligned nanoflakes and fabrication of graphene-like BN by exfoliation*. Journal of Materials Chemistry.
- [3] Kwiatkowska, Barbara. *Stimulation of bioprocesses by ultrasound*. University of Abertay Dundee, 2011. Elsevier, Inc., 2011. Print.
- [4] "Metroline M4L Plasma Etcher - Plasma Etch." *Nanofabrication Laboratory-Materials Research Institute* . N.p.. Web. 30 Mar 2013.  
<[http://www.mri.psu.edu/facilities/nanofab/equipment/plasma\\_m4l/](http://www.mri.psu.edu/facilities/nanofab/equipment/plasma_m4l/)>.
- [5] Tighe, Tim. "Atomic Force Microscopy (AFM) ." *Materials Characterization Laboratory*. N.p.. Web. 30 Mar 2013.  
<<http://www.mri.psu.edu/facilities/mcl/techniques/AFM.asp>>.
- [6] Pittenger, Bede. *Quantitative Mechanical Property Mapping at the Nanoscale with PeakForce QNM* . Veeco Instruments Inc., Print.
- [7] Stapleton, Josh. "Optical Profilometry." *Materials Characterization Laboratory*. N.p.. Web. 30 Mar 2013.  
<<http://www.mri.psu.edu/facilities/mcl/techniques/optProfilometry.asp>>.
- [8] "Dynamic Light Scattering (DLS)." *Malvern*. N.p.. Web. 30 Mar 2013.  
<[http://www.malvern.com/labeng/technology/dynamic\\_light\\_scattering/dynamic\\_light\\_scattering.htm](http://www.malvern.com/labeng/technology/dynamic_light_scattering/dynamic_light_scattering.htm)>.

- [9] Stapleton, Josh. "Ultraviolet-Visible Spectroscopy (UV-Vis) ." *Materials Characterization Laboratory*. N.p.. Web. 30 Mar 2013.  
<<http://www.mri.psu.edu/facilities/mcl/techniques/UV-Vis/UV-Vis.asp>>.
- [10] Lin, Y., Williams, T., Tian-Bing, X., Wei, C., Hani, E., & Connell, J. (2011, January 20). *Aqueous Dispersions of Few-Layered and Monolayered Hexagonal Boron Nitride Nanosheets from Sonication-Assisted Hydrolysis: Critical Role of Water*. The Journal of Physical Chemistry Letters.
- [11] Wang, Y., Shi, Z., & Yin, J. (2011, May 19). *Boron nitride nanosheets: large-scale exfoliation in methanesulfonic acid and their composites with polybenzimidazole*. Journal of Materials Chemistry.

## Academic Vita

### Michael A. Kelly

#### *School Address*

121 S. W. Fairmount Ave. Apt. F16  
State College, PA 16801  
215-595-8619

#### *Home Address*

416 Byerly Dr.  
New Hope, PA 18938  
215-595-8619

**EDUCATION** The Pennsylvania State University- University Park, PA  
*Schreyer Honors College*  
Bachelor of Science in Engineering Science (May 2013)  
*Honors Curriculum in Engineering*

#### **Relevant Courses**

Engineering Design	Circuits and Devices	Speech
Communication	Technical Writing	Heat Transfer
Nanotechnology		

**COMPUTER SKILLS** Solid Works      C++ Programming      Microsoft Office  
MATLAB

#### **WORK AND EXPERIENCE**

**Undergraduate Research Assistant** (October 2011- Present)  
Materials Research Institute, The Pennsylvania State University

- Part of a research team who focuses on the chemical synthesis and characterization of two-dimensional materials for electronic devices.
- Leader of individual research project on the chemical exfoliation of hexagonal boron nitride.
- Worked as Lab Manager for the summer of 2012

**Grounds Department Worker** (May 2011- August 2011)  
Delaware Valley College, Doylestown, PA

- General maintenance of the campus' grounds
- Worked collaboratively in small groups to complete several projects that included lawn mowing, mulching, edging, weeding, etc.

**Farmer's Assistant Worker** (May 2010- August 2010)  
Manoff Market Gardens, Solebury, PA

- Prepared orchards in off-seasons to maintain crop production.
- Picked and counted apples, peaches, blackberries, raspberries, cherries, and nectarines to be sold.

**ACTIVITIES** INFINITY THON (Fall 2011- Present)

**AND AWARDS** Tau Beta Pi, Phi Kappa Phi (Fall 2011- Present)

Jean Kearns McNitt Scholarship in Engineering Science (2011-2013)

Strauss Engineering Scholarship (2010-2011)

Dean's List (Fall/Spring '09, Fall/Spring '10, Fall/Spring '11)